N-TYPE THERMOELECTRIC PERFORMANCE OF FUNCTIONALIZED CARBON NANOTUBE-FILLED POLYMER COMPOSITES

A Thesis

by

DALLAS D. FREEMAN II

Submitted to the Office of Graduate Studies of
Texas A&M University
in partial fulfillment of the requirements for the degree of

MASTER OF SCIENCE

May 2012

Major Subject: Mechanical Engineering

N-Type Thermoelectric Performance of Functionalized Carbon Nanotube-Filled Polymer Composites

N-TYPE THERMOELECTRIC PERFORMANCE OF FUNCTIONALIZED CARBON NANOTUBE-FILLED POLYMER COMPOSITES

A Thesis

by

DALLAS D. FREEMAN II

Submitted to the Office of Graduate Studies of
Texas A&M University
in partial fulfillment of the requirements for the degree of

MASTER OF SCIENCE

Approved by:

Chair of Committee,	Choongho Yu
Committee Members,	David Staack
	Shao Lin
Head of Department,	Jerald A. Caton

May 2012

Major Subject: Mechanical Engineering

ABSTRACT

N-Type Thermoelectric Performance of Functionalized Carbon Nanotube-Filled Polymer Composites. (May 2012)

Dallas D. Freeman, B.S., Brigham Young University

Chair of Advisory Committee: Dr. Choongho Yu

Carbon nanotubes were dispersed and functionalized with polyethylene imine (PEI) before incorporation in a polyvinyl acetate matrix. The resulting samples exhibit air-stable N-type characteristics with electrical conductivities as great as 1600 S/m and thermopowers as high as 100 μV/K. Thermopowers and electrical conductivities correlate, in a reversal of the trend found in typical materials. This phenomenon is believed to be due to the increase in the number of tubes that are evenly coated in a better dispersed sample. Increasing the amount of PEI relative to the other constituents positively affects thermopower but not conductivity. Air exposure reduces both thermopower and conductivity, but a stable value is reached within seven days following film fabrication. The atmospheric effects on the electrical conductivity prove to be reversible. Oxygen is believed to be the primary contributor to the decay.

DEDICATION

To Mrs. Teri Hall, who taught me to say more using fewer words

ACKNOWLEDGEMENTS

I would like to thank my committee chair Dr. Yu for teaching what graduate education is supposed to be. I also thank my committee members, Dr. Staack and Dr. Shao for helping to make this thesis what it is.

Thanks to Kyungwho Choi, also. Without his untold hours of patient instruction and reminders, I would still not know how to produce meaningful, scientific results. I'm grateful also to the other members of Dr Yu's team, each of whom has brightened my time in the lab enough to keep work from turning into drudgery.

Lastly, thanks to my mother for believing I can do anything and for my father for showing me how hard I'd have to work for it. Thanks to my wife and my son for putting up with my absence while I did my research and for always making me glad to come home at the end of the day.

NOMENCLATURE

CNT	Carbon Nanotube
PEI	Polyethylene Imine
SDBS	Sodium Dodecylbenzene Sulphonate
PVAC	Polyvinyl Acetate
S	Thermopower (Seebeck Value)
σ	Electrical Conductivity
wt. %	Weight Percent

TABLE OF CONTENTS

Page

LIST OF FIGURES

FIGURE Page

LIST OF TABLES

1. INTRODUCTION: THE NEED FOR THERMOELECTRIC POLYMERS

The search for energy sources to serve as alternatives to fossils fuels remains one of the most important engineering challenges facing humanity. This broad field includes research into the thermoelectric effect, whereby a voltage difference is produced along a heated material with a polarity running either from the hot side to the cold side for p-type materials or vice versa for n-type materials.

Functional thermoelectric devices can produce electricity anywhere there is a temperature gradient. Conversely, they can be employed as refrigeration devices if a voltage is supplied, creating refrigeration without pumps or fluids. This property, known as the Seebeck effect, was first discovered in 1823 by Thomas Seebeck.[1] Over a century later in the 1950s, it was discovered that semiconductors are better than metals at producing higher voltages per degree of temperature gradient. All known semiconductors were evaluated as potential generators before it was determined that a combination of bismuth telluride and bismuth antimony alloys prove the most efficient.[2] These alloys have coefficients of performances of about 1/3 those of typical home refrigerators, limiting potential applications to those where longevity, space requirements and quiet operation are of greater importance than efficiency.[3]

Starting in the 1990s, research into thermoelectric materials has continued and improvements have been made to the efficiency of the bismuth alloys through control of

---

This thesis follows the style of *ACS Nano Letters.*

the material properties at the nano scale.[2] Other materials are also being reevaluated using these new techniques. Potential applications include energy reclamation in existing generators, improvement of efficiency in solar cells, portable refrigeration units and active cooling of computer processing chips.

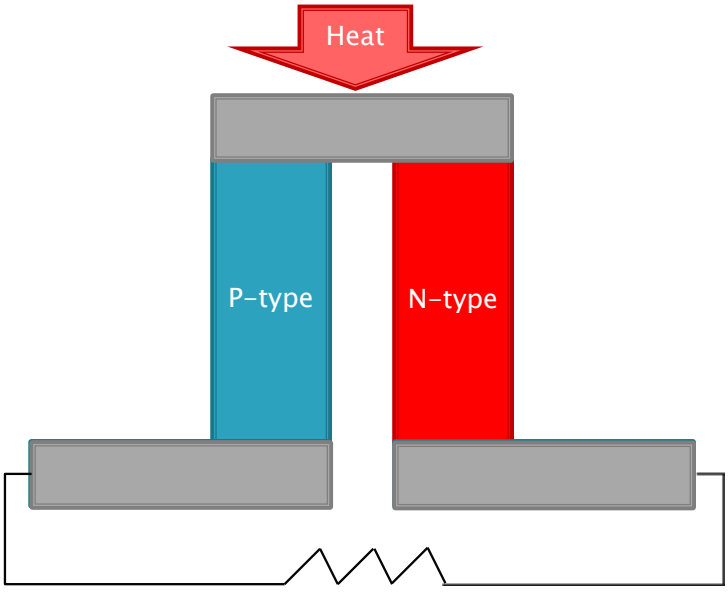

Figure 1. Schematic of a thermoelectric generator with legs containing positive charge carriers (p-type) and negative charge carriers (n-type).

A thermoelectric device consists of two semiconductor legs connected in series electrically and in parallel thermally (Figure 1). The n-type leg uses electrons as the primary charge carrier, while the p-type charge carrier is a theoretical construct describing an electron vacancy known as a hole, which has a charge equal and opposite

to that of an electron. While either n-type or p-type thermoelectric materials produce voltages in the presence of temperature gradients, a working thermoelectric device employs both n- and p-type components in order to maximize current flow.

The thermoelectric figure of merit, used to describe the thermoelectric effectiveness of any material, is given by

$$Z = \frac{S^2\sigma}{\kappa} \tag{1}$$

where S is the thermopower, σ is the electrical conductivity and k is thermal conductivity.[4] Thermopower, also known as the Seebeck value, is a temperature-dependent measure of how much voltage a thermoelectric material generates divided by the temperature difference needed to produce it.[3] The Seebeck value is generally high in insulators and low in metals. Electrical and thermal conductivity are, conversely, low in insulators and high in metals. As can be seen from Equation 1, a good thermoelectric material will have a high electrical conductivity so that charge carriers, energized by the heat flowing into the hot side of the material, can have the mobility to move towards the cold side, creating the potential difference. The good thermoelectric material will also have a low thermal conductivity, so that the temperature gradient between both ends is maximized. Semiconductors are typically used because charge carriers move freely through the bulk material, resulting in a higher electrical conductivity than thermal insulators. However, the reduced amount of free charge carriers relative to metals leaves most of the thermal energy conducted not by electrons, as in metals, but by slower

moving atomic lattice vibrations, or phonons, which results in a lower thermal conductivity.[5]

Since their discovery in 1991, carbon nanotubes (CNTs) have been extensively studied as potential solutions in a wide range of applications due to their unique mechanical, electrical and geometric properties.[6] Many of the tubes, which are composed of one or more rolled sheets of the carbon honeycomb structure known as graphene, are semi-conductive depending on the lattice vector by which they are rolled. Intrinsically n-type, semiconducting nanotubes are highly susceptible to oxygen doping and become p-type in atmosphere.[7]

Several methods have been demonstrated for the production of air stable n-type nanotubes, including passivation of a protective film around the tubes to prevent oxygen doping, application of viologens for a direct redox reactions, and the use of metal electrodes with low work functions.[8-10] A simpler production method has also been demonstrated wherein the physical adsorption of branched polyethylene imine (PEI) onto carbon nanotubes results in a conversion of the tubes' conducting properties from p-type back to n-type.[11] Nanotubes functionalized with PEI have been been used to produce p-n junctions, photovoltaic cells, and field-effect transistors[11-14] In our previous work, the thermopower of thin films composed of PEI-doped tubes was measured to be as high as 60 μV/K.[15] Such films, composed almost purely of carbon nanotubes, are not prime candidates for thermoelectric generation because their thermal energy transport is too high, and because they are physically bound to a rigid, thermally insulating substrate.

A few years after their discovery, CNTs were first incorporated into a polymer matrix for the purpose of electrical doping.[16] It was determined that the electrical conductivity of these composites are best described using percolation theory, wherein nanotubes form a network of conductive filler within the composite.[17] The ability of energy carriers to move along this network is the limiting factor for the conductivity of the composite. Such composites have since been researched extensively for a variety of applications.[16] Effort has been made to reduce the percolation threshold, or the required weight percent of CNTs required for a network to form.[18] The goal is to reduce cost while maximizing mechanical and electrical properties of the final composites.

CNT/Polymer composites have been evaluated for their thermoelectric properties.[19] Although thermal and electrical conductivities are usually correlated, these composites exhibit electrical conductivities nearly as high as films composed exclusively of tubes, but still possess thermal conductivities closer to those their polymer matrices. This phenomenon results from the relative ease with which charge carriers travel across the nanotube network. The thermal carriers, or phonons, have relative difficulty with transport because they are scattered at the CNT surfaces and at the junctions between the tubes, limiting the speed at which they cross the bulk material.[18] The result is a material with high electrical conductivity, low thermal conductivity, and a resulting high thermoelectric figure of merit. P-doped composites have been produced which exhibit electrical conductivities as high as 10^5 S\m .[19] While several studies have been conducted on carbon nanotube/polymer composites, none of them have investigated the

thermoelectric properties of such polymers when the nanotubes are converted into air-stable n-type.

2. EXPERIMENTAL

Single and double walled carbon nanotubes, made using combustion carbon vapor deposition by CheapTubes Inc., were used for the experiment. The mixture of single and double walled tubes was approximately 50/50 with tube diameters and lengths of 1-2 nm and 3-30 μm respectively. The manufacturer claimed 90% purity for the first batch of tubes, having eliminated almost all of the catalyst and amorphous carbon materials. The second batch was rated at 99% purity.

For each experiment, 60 mg of Carbon Nanotubes (CNTs) were dispersed in between 5 to 15 ml of deionized water with a prescribed amount of the surfactant Sodium Dodecylbenzene Sulfonate (SDBS). Sonication was conducted in two modes. The first was to sonicate using the XL-2000 pen-type sonicator from Misonix for 15 minutes and for additional 15 minutes on the FB 120 from Fisher. The other mode was to use the Branson 1510 bath type sonicator for 24 hours (Figure 2).

Figure 2. Bath type (left) and pen type (Right) sonicators used for dispersion.

Afterward, a determined amount of 5% water solution of PEI was added with a pipette into the dispersion. It has been demonstrated that PEI attaches to nanotubes by physisorption on the tube sidewall.[20] To maximize the occurrence of physisorption and create an even coating of PEI on the nanotubes, the dispersions were stirred for 48 hours while being maintained at a temperature of 50-60 ° C. The prescribed amount of polyvinyl acetate, Vinnapas 401 (Wacker Polymers), which had been diluted in water for ease of measurement, was subsequently added into the dispersion. The nanotubes were dispersed by both pen-type sonicators for 30 minutes each and then cast using a 5 cm x 5 cm x 2 cm plastic container as a substrate (Figure 3). Films 20-80 μm thick formed as the dispersion dried, in a process that usually took between 24 and 48 hours. Dried

samples were then thermally annealed in a vacuum oven at 60° C for 4 hrs. to any water which had permeated the film (Figure 4).

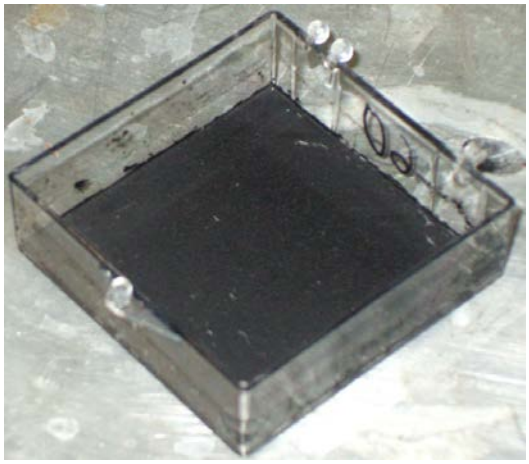

Figure 3. Dried composite film in container.

Figure 4. Drying was completed in a vacuum oven.

Three series of samples were run. In the first, the weight percent of SDBS was varied while the weight percentages of CNT and PEI were maintained at 20 and 10 wt. %, respectively. The second series consisted of two parts, one of which varied PEI wt. % while maintaining SDBS and CNT both at 20 wt. % and the other which did the same except that SDBS was held at 40 wt. %. All weight percentages were determined by measuring the mass of the material on a scale before including it in the sample. The weight percent Vinnapas was varied in each series to make up whatever difference was left between the total of the other three weight percentages and 100 percent. A summary of the experiments is included in Table 1.

It should be noted that a certain amount of variability was necessarily tolerated. For example, the oven treatments were sometimes as little as 3.5 hours, and the sonication times may have been reduced or lengthened by as much as 10% percent. More controlled experiments would probably result in less variability, but the nanotube production and the composite formation procedures themselves will need to advance significantly for consistency to reach commercially acceptable levels.

Table 1 Summary of preparation conditions for three series run.

Series	CNT	SDBS	PEI	PVAC
1-1	20	20	10	50
1-2	20	40	10	30
1-3	20	60	10	10
1-4	20	60	10	10
1-5	20	40	10	30
1-6	20	20	10	50
1-7	20	60	10	10
1-8	20	60	10	10
2-1	20	20	40	20
2-2	20	20	20	40
2-3	20	20	10	50
2-4	20	20	5	55
2-5	20	20	40	20
2-6	20	20	50	10
2-7	20	20	50	10
2-8	20	20	50	10
2-9	20	20	10	50
2-10	20	20	20	40
2-11	20	20	30	30
2-12	20	20	40	20
2-13	20	20	50	10
3-1	20	20	10	90
3-2	20	20	20	40
3-3	20	20	30	50
3-4	20	20	10	20
3-5	20	20	20	10
3-6	20	20	30	10
3-7	20	20	40	10
3-8	20	20	40	50
3-9	20	20	10	40
3-10	20	20	40	30

After fabrication, each sample was tested for conductivity and Seebeck value. To this end, a rectangular test sample of the dried and annealed film was removed from the plastic container. Conductive silver paste was applied to the sample strip to minimize electrical and thermal contact resistance and the relevant dimensions were measured using a micrometer (Figure 5).

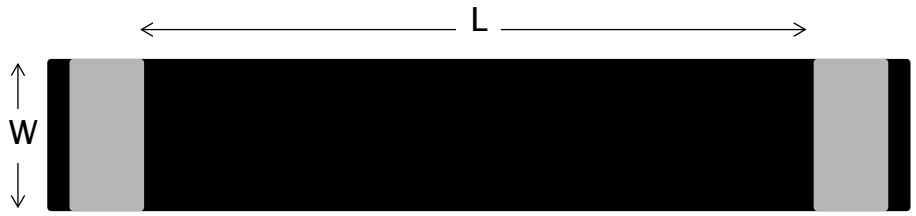

Figure 5. Diagram of electrical testing strip with conductive silver paint applied.

A four point probe resistance measurement was run, scanning 20 data points with ranges of plus or minus 4, 7 and 10 volts. Figure 6 show an example measurement where the resistance value is 80 Ω. After the resistance was measured, the sample conductivity was calculated from the resistance and dimension values with:

$$\sigma = \frac{L}{R \cdot w \cdot t} \tag{2}$$

Where σ is the electrical conductivity, *R* is the average resistance from the three ranges, *L* is the distance between the edges of the conductive strips and *w*, and *t* are the width and thickness.

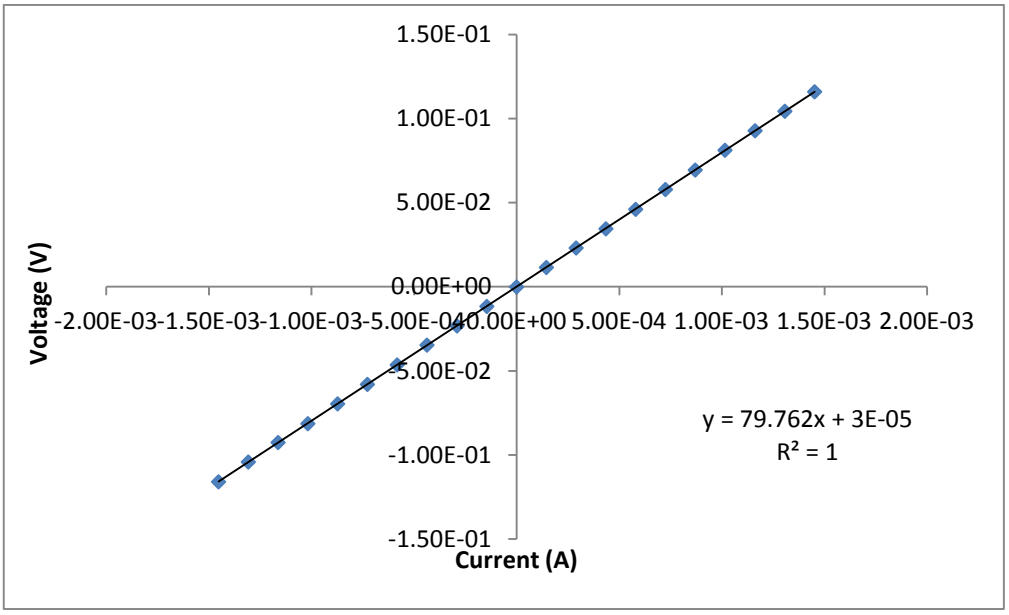

Figure 6. Sample data series for resistance measurement. Three data sets where run for each measurement with voltages varying from plus or minus 4, 7, and 10 volts.

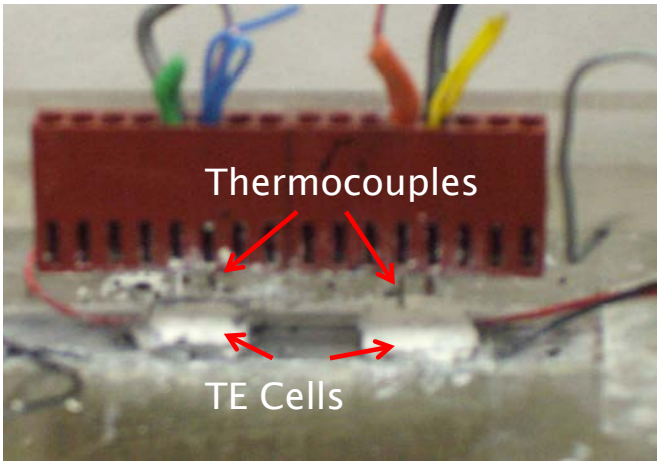

Figure 7. Test apparatus used to measure electrical conductivity and thermopower.

The Seebeck value was measured using a Keithley 2400 multimeter controlled by a data acquisition device from National Instruments. On average, eight temperature differences were measured using thermocouples placed at either end of the sample. Voltage differences between the two thermocouples were then immediately measured. The thermopower was calculated as the slope of the linear regression line formed using the temperature differences as the dependent variable and the voltage differences as the independent variable. Figure 8 is an example of one measurement where the thermopower is equal to 60μV/K. It was here that the determination of main carrier type was made, as the negative thermopowers of n-type materials will result in a positive slope for this graph. This slope maintains its sign even if the probe polarities were reversed, as doing so would change the signs of both the voltage and the temperature gradient, cancelling any sign change.

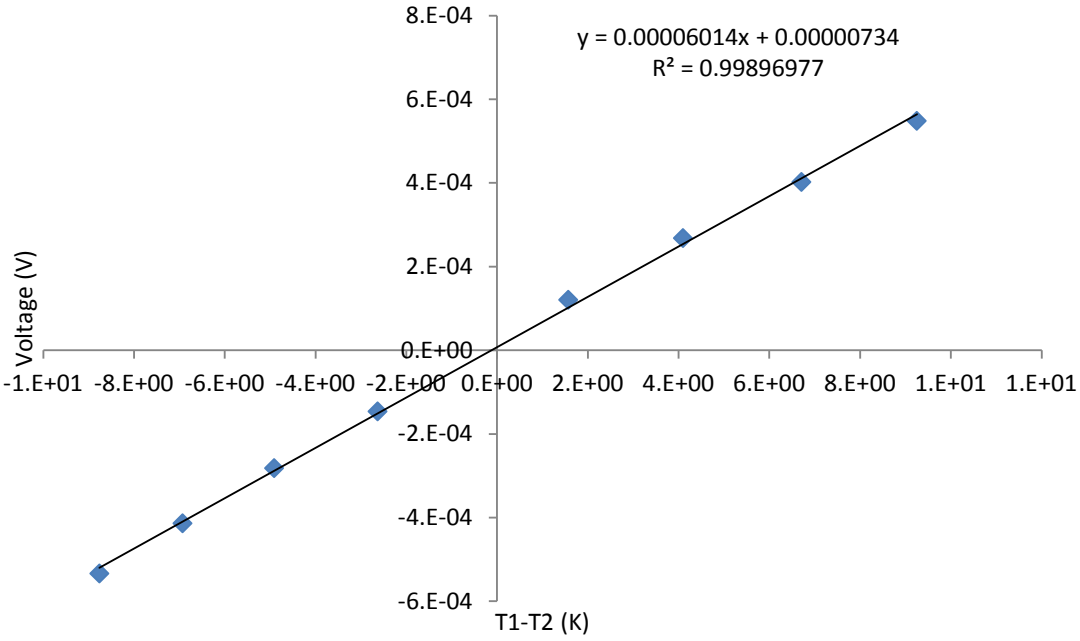

Figure 8. Typical data set used for calculation of thermopower. The positive slope indicates the sample is n-type.

After the initial test, several samples were tested at different times to determine how the properties would change. Additionally, select samples were cold fractured in liquid nitrogen. Scanning electron micrographs were taken of the cold fractured edges for the purpose of examining the relationship of the micro-scale structures and the electrical properties that were measured.

3. RESULTS AND DISCUSSION

Dispersion remains a primary consideration in the production of CNT composites, whether structural or electrical.[21] In this work, the surfactant SDBS was chosen to facilitate dispersion based on its superior performance and for its tendency to form smooth coating layers around the CNTs.[22, 23] The principle challenge specific to this research resulted from the use of polyethylene imine. PEI is the polymer dopant which donates electrons to the nanotubes, making them air-stable n-type semiconductors. The polymer contains one of the highest densities of amine groups of all polymers, (Figure 9) and it is these which donate their electrons to the carbon nanotubes.[15]

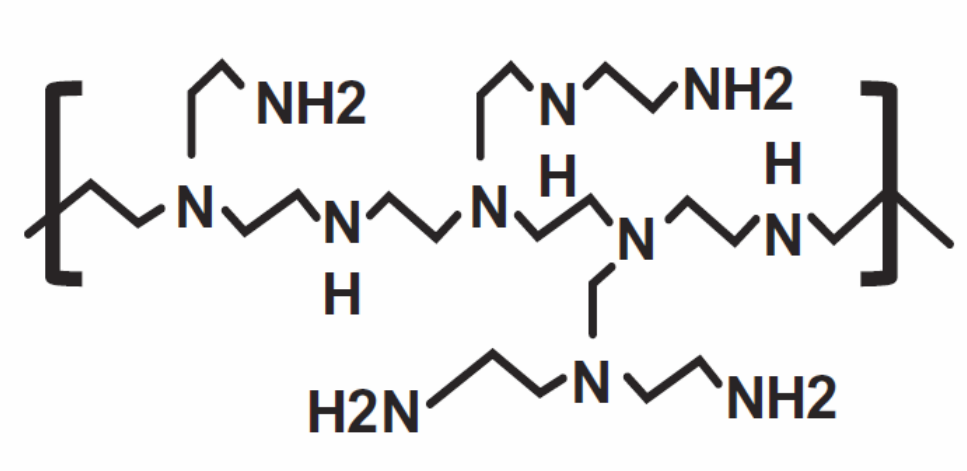

Figure 9. Structure of branched PEI

The PEI used in this study had an average molecular weight of 1800, indicating that it was composed of molecules that were made of four units like the one shown in Figure 9. Although covalent bonding has been demonstrated for the case of F-functionalized (fluorinated) CNTs, pristine CNTs like those used in this study will interact with PEI via physisorption.[23] In this process, the PEI molecules wrap around the CNTs and form bonds other PEI molecules or with the opposite ends of the molecule. It has been shown with AFM imaging that this coating of PEI molecules causes the tube to double in diameter relative to uncoated tubes.[24] In previous experiments where the tubes were soaked in PEI solutions, filtered rinsed and allowed to dry, the doped tubes were heavier than they were before being added to the solution. This finding is especially intriguing given the expected loss of tubes in the filtering and rinsing processes which have been observed in the lab to be about 25%. This increase in volume and mass indicates a need for more intense sonication than is required for pristine tubes.

Essential as it is to produce the desired n-type polymers, PEI also acts as a coagulant for CNTs in water which can counteract the effects of the surfactant.[25] Even high quality dispersions in water were observed to form agglomerations of tubes if too much PEI was added. Acceptable mechanical properties were attained by Muñoz et al. with nano-sized spun fibers containing 75 wt. % nanotubes and 25 wt. % PEI.[25] In my study, similarly low concentrations of PEI produced composites with good mechanical properties. However, as the concentration of PEI increased to 50 wt. %, the samples were qualitatively observed to have lost elastic modulus and ultimate strength. This effect is attributed to the difficulty PEI adds to the dispersion process, and to PEI's room

temperature liquid state. Experiments using a stronger matrix polymer, one capable of mitigating these undesirable mechanical effects, may prove useful.

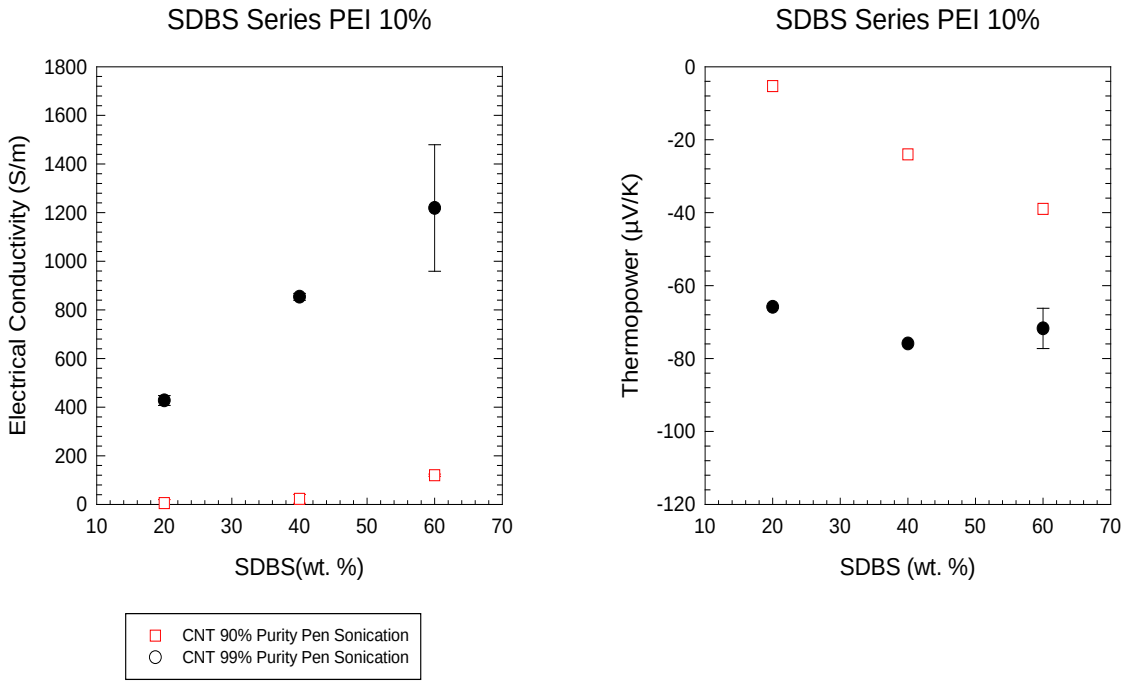

Figure 10. Change in properties as a function of surfactant weight percent. Correlation is positive for thermopower magnitude and electrical conductivity.

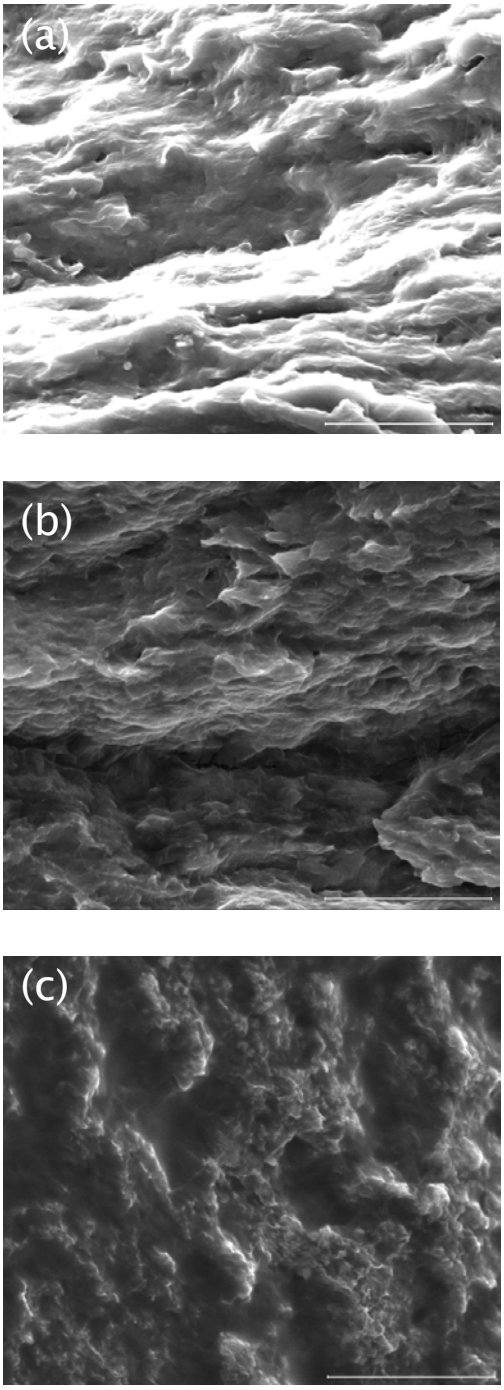

Figure 11. SEM images of cold fractured surfaces for samples with 20 wt. % CNT and 60, 40, and 20 wt. % SDBS (a, b, and c respectively.) Fractures become increasing sharp and disorganized as less surfactant is included, eventually forming non homogenous structures as seen in (c).

The first series revealed correlation between SDBS and both thermopower and electrical conductivity (Figure 10). This correlation is readily understandable in the case of conductivity. As shown in the SEM images for three samples of different conductivities (Figure 11), the samples with higher SDBS weight percent exhibit smoother cleavages and fewer CNT pullouts. Both of these are characteristics of good dispersion, indicating that SDBS weight percent at a ratio of 3 to 1 with CNT is more effective at deconstructing the bundles than smaller ratios. As the amount of SDBS goes down, the CNTs agglomerate more, forming networks around internal voids like those shown in Figure 11 c. Being insulators, voids such as these will reduce overall electrical conductivity for the composite. Figure 10 also demonstrates a large difference between tubes rated as having 99% purity and those at 90%, probably due to the lower conductivity of amorphous carbon and the catalyst impurities.[26] The heavy catalyst particles may also have a negative effect on dispersion, forcing tubes to which they are attached to fall into a precipitate.

The correlation of thermopower and electrical conductivity warrants discussion. The opposite situation is found in most material systems where thermopower and conductivity have an inverse relationship, explained qualitatively by the fact that an increased amount of charge carriers will drive down the voltage potential being induced by the temperature gradient.[2] Even p-doped carbon nanotube composites follow the inverse trend.[27] The effects observed in this work can be explained in a number of ways. The first hypothesis involves the thickness and the aggregation of tube bundles. Studying Figure 11, one notices that, as SDBS increases, surface roughness increases

with it and, in the case of the third sample, there is also a formation of a heterogeneous microstructure of tubes running around voids which appear as the dark, smooth areas on the image. This increase in composite heterogeneity can have negative effects on electrical conductivity and thermopower via at least two modes. The first is a reduction in electron pathways through the material. Fewer pathways mean that the composite as a whole will have less conductivity than a material where the tubes were more completely dispersed (Figure 12). This is the explanation offered for results involving a similar system where epoxy was the polymer matrix used.[28] Conversely, a decrease in the number of nanotubes in each bundle results in an increase in the amount of tubes coming into physical contact with the PEI molecules, allowing for more effective doping as fewer of the tubes from the center of the bundles are allowed to remain P-type and reduce the magnitude of the composite Seebeck value. This is illustrated schematically in Figure 13, though it is important to note that the actual bundles contain dozens to hundreds of tubes, greatly limiting the effect of PEI on tubes in the interior of the bundles.

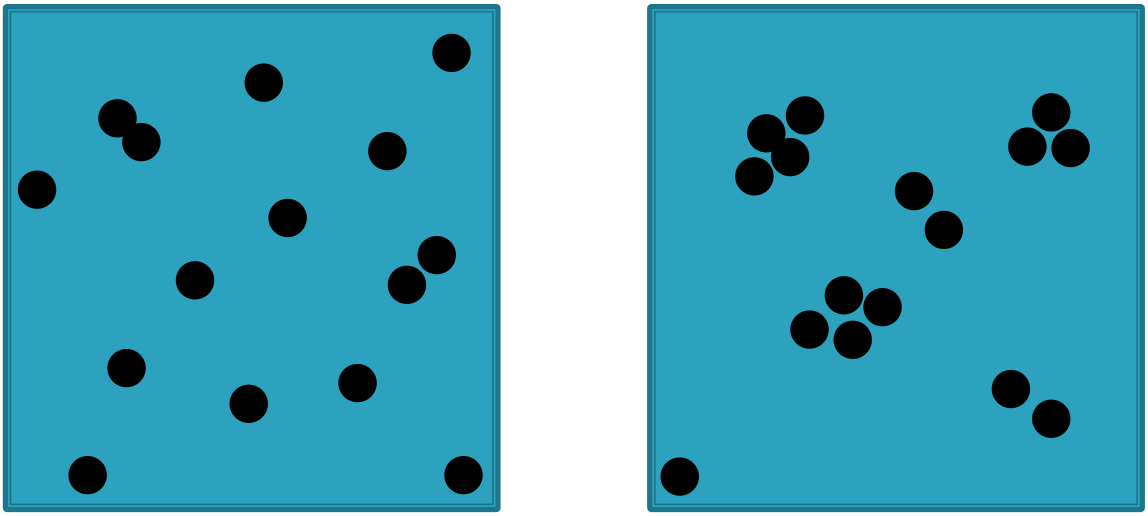

Figure 12. CNT bundles cross sections in composites with good dispersion (left) and bad dispersion (right).

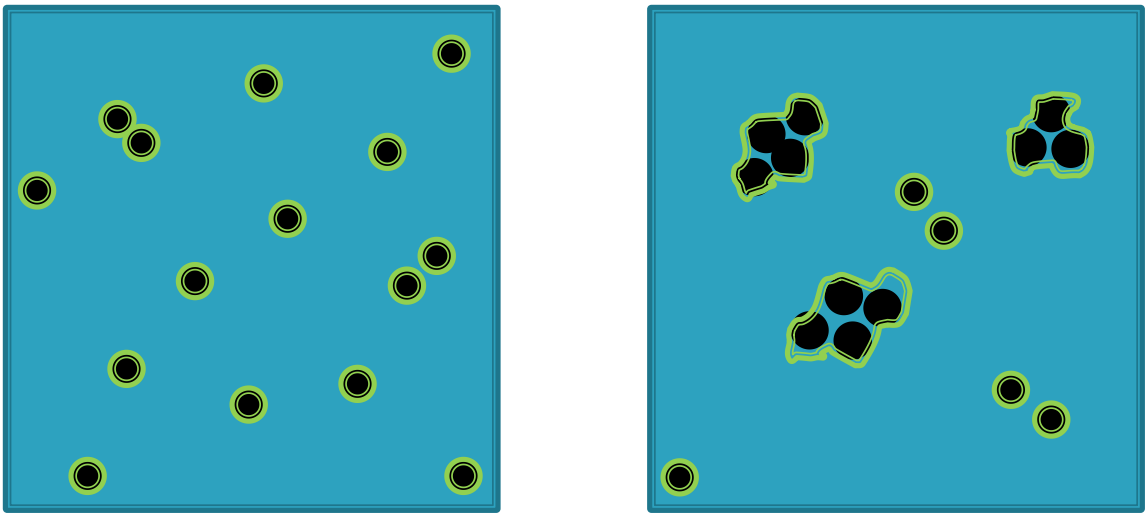

Figure 13. How poor dispersion limits the physical contact of PEI molecules (green) with carbon nanotubes when they form part of large bundles.

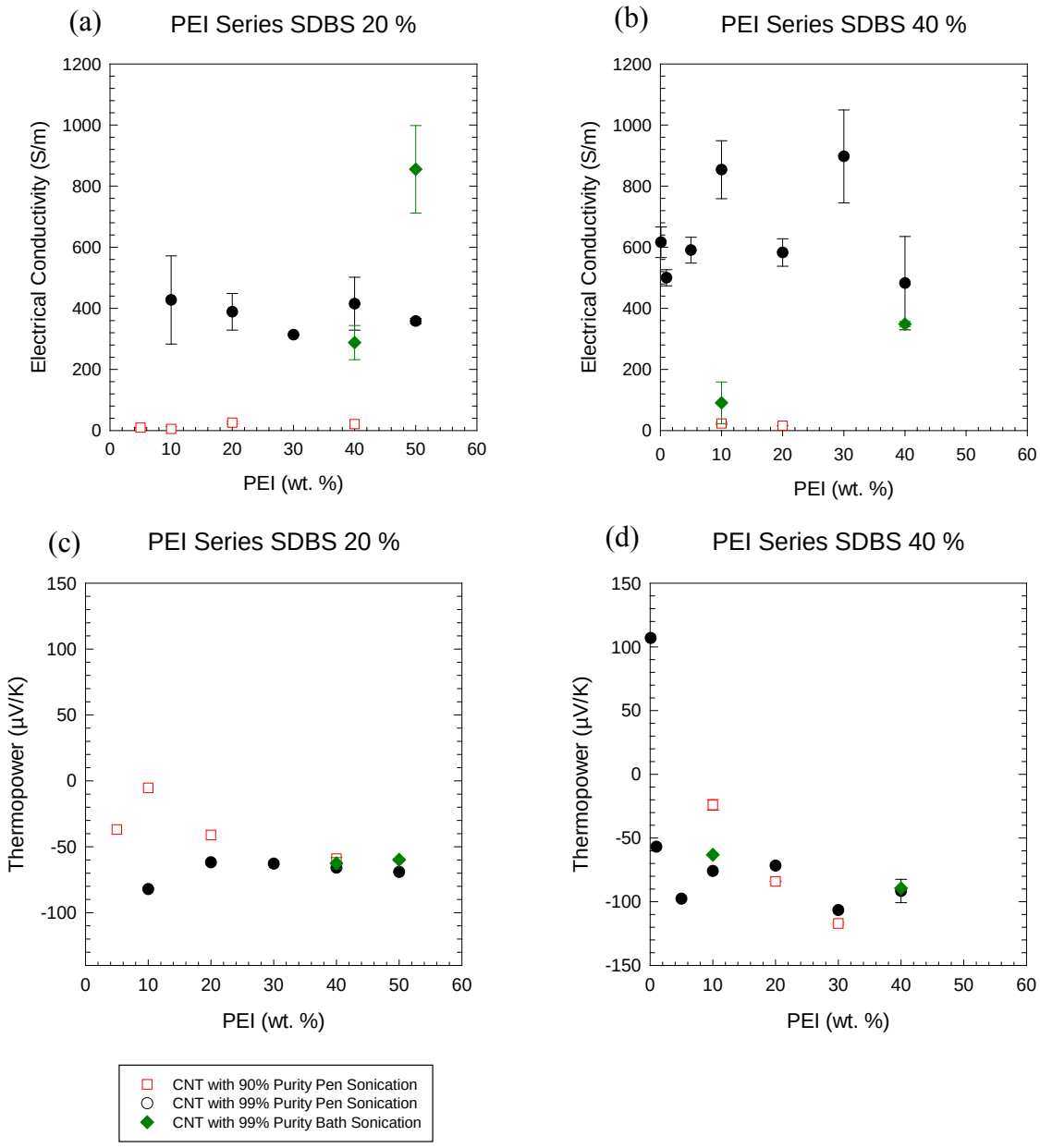

Figure 14. Effect of weight percent of PEI on properties for samples containing 20 wt. % SDBS (left) and 40 wt. % (right)

A review of the results of the second and third series (Figure 14) is now undertaken. The first item to note is the lack of consistent difference between bath

sonication (green diamonds) and pen type sonication (red squares and black circles). The lack of effect was somewhat surprising as unpublished findings in the lab with CNTs undergoing treatments different from the ones in this study have shown that the prolonged exposure to the lower power ultrasonic waves generated by the bath sonicator produce superior dispersions. This does not generally appear to be the case for the samples studied, with the notable exception of the 50 wt. % sample in series two, where the electrical conductivity is higher than those of surrounding samples. This single point is, of course, proof of nothing, but there is reason to believe that if such variables as the dispersion temperature, the amount of water used in fabrication and the relative levels of the water inside the container and the water in the bath were carefully controlled, bath sonication has the potential for superior dispersion without the inclusion of large amounts of SDBS.

It should be noted that the error bars for the two bath-sonicated samples in series two represent multiple samples, prepared using the same conditions at different times. This is also the case for the highest SDBS wt. % sample in series one. For all other samples, the error bars are a result of measurement uncertainty, with the largest contributor being the difficulty in precisely measuring the thickness using calipers, given that the samples are often highly compressible.

Aside from the uncertainty in the measurement, the trends clearly show a high level of variability. This could be owed to any number of things which were not controlled during the experiment. These include humidity and the temperature of the sample during drying, as well as such sonication conditions as probe position relative to

the container and whether or not the container was held in place or allowed to slide as its contents were exposed to vibration. As discussed earlier in this section, the presence of PEI increases the difficulty in producing useful composites and approximately 10 % of sample attempts failed to produce a testable film. In the future, greater effort should be made to control as many of these conditions as possible to reduce variability and observe trends. That aside, the data we currently have does provide access to several insights.

The two PEI series do not reveal a correlation between electrical conductivity and PEI weight percent at the levels studied. The first three levels of series two (0.1, 1, and 5 wt. % PEI) demonstrate a positive correlation between PEI weight percent and thermopower. The sample containing only 0.1 wt. % has a p-type thermopower comparable to control samples made without incorporating PEI. The 1 wt. % sample exhibits n-types properties of lower magnitude. Above 5 wt. %, the samples demonstrate only a slight correlation with thermopower and additional PEI weight percent, with thermopowers comparable and opposite to the tubes which were not doped. M. Shim et al. estimated the doping fraction of PEI on CNT to be between 1-6 x 10^{-3}. [11] The ratio of the weight percentages of PEI to those of CNT varies in this study from 5 x 10^{-3} to 0.5. Given the average atomic weight of the PEI used, (1800 AMU) and the average dimensions of the carbon nanotubes (see experimental section) it can be calculated that, for these experiments, the ratio of PEI's n-doping amine groups to CNT's carbon atoms ranges from 1 x 10^{-3} to 0.1. Therefore, the failure of the sample containing the lowest level of PEI to convert to n-type is not unexpected, as the amount used was at the lowest reported doping ratio. This is especially true when one considers that M. Shim measured

the amount of PEI molecules which had actually attached to the nanotubes, whereas, in this study, it can be assumed that dopant molecules were evenly dispersed throughout the composite, many of them not even coming into contact with CNT. The value for the thermopower of the 1 wt. % PEI sample supports this hypothesis that the PEI molecules are evenly dispersed. Assuming an even dispersion of PEI throughout the composite, it can be estimated that in these samples, which all contain 20 wt. % CNTs, somewhere around 20% of the PEI molecules used would occupy positions in useful proximity to the CNTs. The second sample could be estimated to have a doping ratio of 5×10^{-3}, a value within the ranges of the ratios measured by Shim et al.

More analysis will be required to determine whether the PEI aggregates around the tubes or distributes itself evenly throughout the composite. A good starting point would be to maintain the CNT:PEI weight percent ratio seen in this second sample of 1200 while varying the weight percent of CNTs. If the thermopower remained consistent for the various samples, this would provide evidence that PEI attaches to the CNTs preferentially over SDBS and PVAC molecules. If the thermopower decreased with increasing CNT concentration, there would be additional evidence supporting even distribution within the sample.

Saturation beyond 10 wt. % PEI is to be expected. At this point, there simply ceases to be room for any additional PEI to attach. However, series three does reveal a weak correlation between PEI weight percent and thermopower, and this phenomenon does bear an attempt at explanation.

Key to the hypothetical explanation for this behavior is the improved thermopower and the lack of effect on electrical conductivity which is observed for the third series. Such behavior has been observed to result from a phenomenon known as energy filtering.[2] The following equation for thermopower will be useful to the explanation.

$$S = \frac{1}{eT} \frac{\int \nu^2 \tau (E - E_f) \frac{\partial f_o}{\partial E} D(E) dE}{\int \nu^2 \tau \frac{\partial f_o}{\partial E} D(E) dE} \tag{3}$$

Here, *e* is the charge on the electron, *T* is the temperature, ν is the average electron velocity, τ is the relaxation time, f_0 is Fermi-Dirac distribution, and D(E) is the density of states.[11] In simplest terms, thermopower is the measure of the average carrier energy above the Fermi level $(E - E_f)$. Any increase to this average will increase the thermopower.

Within the composite, nanotubes form junctions from one tube to the other. These junctions serve as potential barriers, blocking low energy carriers and raising the average energy of the carriers which make it across the bulk material (Figure 15).[29]

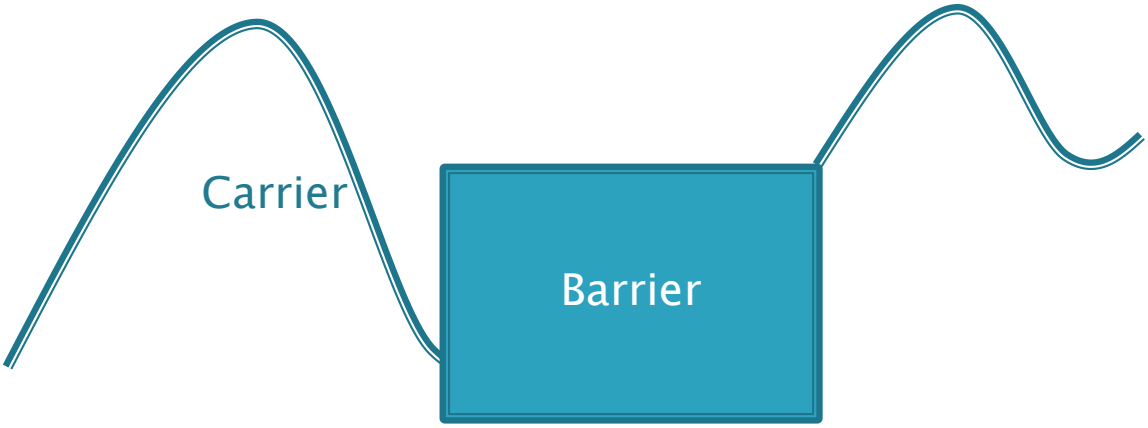

Figure 15. Effect of low energy barrier on average carrier energy

The observed effects of the dispersion on thermopower can be understood along these lines. As the bundles become better dispersed, each carrier encounters more of these junctions, effectively increasing average carrier energy and therefore thermopower (Figure 16). This increase is greater than the loss in electrical conductivity due to the added resistance of the additional junctions. This provides one explanation for the results seen in the third series.

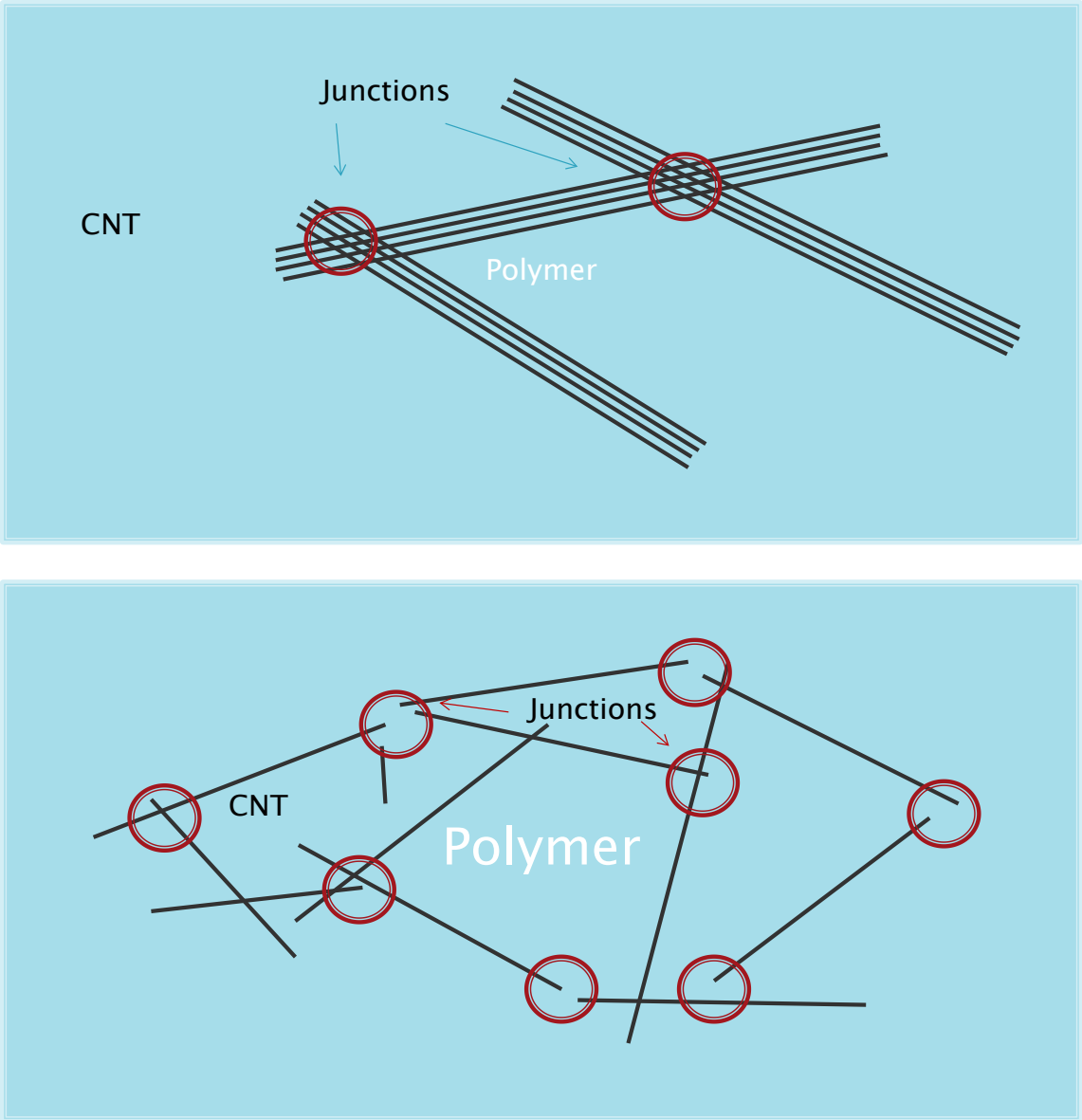

Figure 16. Effect of dispersion on the number of junctions within a conduction network

Comparing the results of series two and three, the average conductivities for each were 380 S/m for series two and 660 S/m for series three. A similar improvement of the thermopower is achieved. (Compare A with B and C with D in Figure 14.) This is an observation of the same effect observed in the first series. Originally, it was thought that the insulating surfactant would adversely affect electrical conductivity by creating an insulating layer between adjacent tube bundles. However, far from being deleterious, the weight percent of surfactant had a much stronger positive effect on the composites' thermoelectric properties than the amount of n-type dopant used because of its favorable effects on nanotube dispersion. This is an illustrative example of the difficulty involved with predicting the thermoelectric behavior of even seemingly simple composite materials systems. Moving forward it will be useful to see if this increase in performance is correlated with the ratio of the weight percentages of SDBS to CNT as assumed or if it is more strongly tied to the concentration of SDBS in the water solution

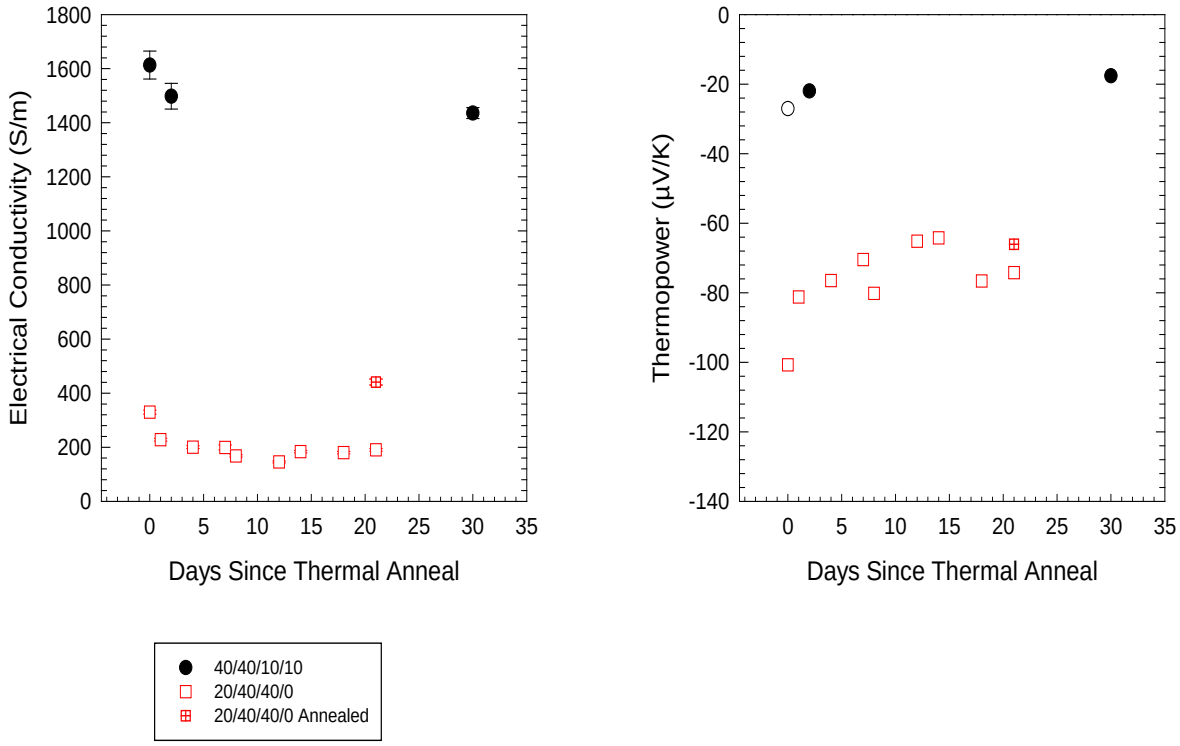

Figure 17. Change in properties as a function of time after vacuum annealing for select samples. The point labeled "20/40/40/0" underwent an additional vacuum annealing on day 21, restoring its electrical conductivity to the original value.

The effects of air on the samples over time are illustrated in Figure 17. The values of conductivity and the thermopower both decay somewhat in the presence of air, owing to the increased levels of oxygen doping on the material. The effects on electrical conductivity were also found to be completely reversible through an additional vacuum annealing process of four hours at 60 ° C (see 20/40/40/0 Annealed). The simultaneous reduction in conductivity and thermopower can be understood in terms of a mixed carrier model, where a conductor uses both electrons and holes as charge carriers. In this situation, the conductivity of the material is governed by

$$\sigma = \sigma_h + \sigma_e \tag{4}$$

Where σ_e and σ_h are the conductivities due to electrons and holes, respectively.[11] The model applies to the current research for a number of reasons. The first is that CNTs exhibit different electrical properties depending on their chirality, or the arrangement of the graphene hexagons relative to the tube axis. These electronic differences can make individual tubes more or less responsive to doping, in addition to making them metallic or semiconducting. In addition, because each nanotube bundle in the composite studied will theoretically be composed of n-type tubes on the outside where the PEI is attached while the tubes inside the bundle will maintain their initial oxygen-induced p-type state, the entire composite is a mixture of p- and n-type charge carriers. The sample as an aggregate exhibits n-type characteristics when σ_e in equation 4 exceeds σ_h.

As the sample is left exposed to the atmosphere, more oxygen molecules will infiltrate the polymer and remove more electrons from the tubes (Figure 18). This reduces σ_e more than it increases in σ_h equation 4, and the overall conductivity is reduced. It should be noted that in the case for pristine n-type nanotubes in vacuum, air exposure results in an increase of conductivity, as oxygen donates sufficient holes to overcome the loss in electrons.[30] This suggests that PEI not only reverses oxygen's p-type doping, but provides CNTs with more electron carriers than they had originally.

A similar explanation can account for the simultaneous loss in thermopower magnitude. The relevant equation is

$$S = \frac{S_e\sigma_e + S_h\sigma_h}{\sigma} \tag{5}$$

Where S_e is the thermopower due to electrons, (having a negative value,) and S_h is the value for holes.[15] As can be seen, a reduction in conductivity due to electrons will decrease the overall thermopower. Once again, changes in electrical conductivity track with changes in thermopower. The mixed carrier model is a likely explanation.

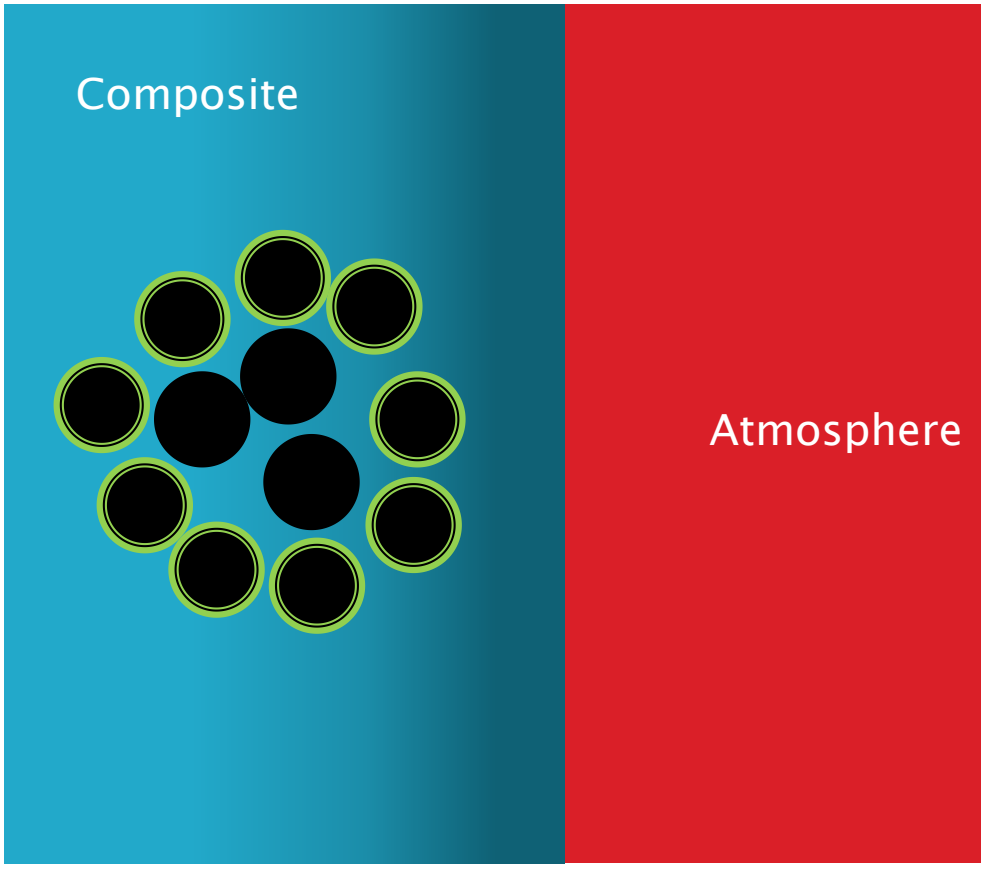

Figure 18. The effects of atmospheric doping on CNT bundles

Additional samples were created besides those that fit into the three series discussed thus far. Most notably, a sample containing 40 wt. % CNTs, 40 wt. % SDBS, 10 wt. % PEI and 10 wt. % PVAC was created twice, exhibiting electrical conductivity of 1600-3100 S/M and thermopower of approximately -40μV/K. The electrical conductivity is much higher than those of the samples containing only 20 wt. % CNT, which is probably due to the increase in electron paths available at higher concentrations. The thermopower is lower than is typical for the three series, this could possible indicate that at higher concentration of CNTs, the atypical correlation of thermopower and electrical conductivity no longer applies. Unfortunately, further research into films containing large weight percentages of CNTs is hampered by the need to maintain a ratio of one to one with CNT and SDBS.

Still, now that it is determined that a sample containing 5 wt. % of PEI performs as well as one containing much more, it may be advisable to run additional experiments using higher concentrations of CNTs with lower concentrations of PEI. In addition, now that the recipe used in samples 1-8 and 1-4 has been determined to produce the most favorable results, two more series should be run where the CNT weight percent is varied. In the first, the SDBS and PEI weight percentages should be maintained as they are in 1-8 and 1-4, and in the second, the ratio of CNTs to these two constituents should be preserved. A comparison of the two may yield insight into the arrangement of the molecules within composite as well as aid future researchers in determining the most economical amount of CNTs to use, balancing energy efficiency with overall cost.

During the course of this research, other tubes besides those produced by CheapTubes Inc. were tested. These included tubes from PS2, CCNI and Unidym. Billed as having higher quality, with fewer imperfections and having proven to produce composites with higher p-type electrical conductivities than those from CheapTubes, these tubes failed to undergo n-type conversion. Though an explanation as to why would be purely hypothetical, it may have to do with the observed tendency for CNTs with a higher concentration of imperfections in their sidewalls to be more reactive and responsive to functionalization. (Srivastava 1999) The idea here is that the carbon atoms at these sites at bonded with their neighbors in a way that is energetically unfavorable. This increases their tendency to bond with molecules capable of functionalizing them. While this may or may not be a valid explanation for the failure of the other brands of CNTs to undergo n-type conversion, the fact remains that while other CNTs have been shown in other labs to respond to PEI-doping, I can only claim success with CheapTubes.

4. CONCLUSION

Air-stable n-type thermoelectric polymer composites were created using carbon nanotubes functionalized with PEI. Thermoelectric properties were measured. Weight percentages of SDBS correlated positively both with thermopower magnitude and electrical conductivity. This was hypothesized to be the result of an increased number of carrier paths in the case of conductivity. In the case of thermopower, the affect was likely due to an increased surface area available for doping interactions. It was determined that increasing the amount of weight percent of PEI will only correlate with thermopower if the amount of PEI is below 5 wt. % and above this only if the nanotubes are sufficiently dispersed within the matrix. This was hypothesized to be the result of energy filtering. The effects of oxygen doping over time were observed and determined to be in keeping with a mixed carrier model.

In the future, studies could be conducted to determine the percolation threshold of the composites by reducing the concentration of CNT and maintaining the ratios between CNT, PEI and SDBS. Different, stronger matrix polymers could be used to combat the deleterious effects of PEI on composite mechanical properties. Eventually, a working combined p and n type cell should be fabricated and evaluated for the thermoelectric figure of merit. This work will pave the way for lightweight, non-toxic and flexible thermoelectric cells capable of harvesting thermal energy from the human body, solar cells and a host of other areas where it is currently going to waste.

REFERENCES

(1) Mahan, G.; Sales, B.; Sharp J. Thermoelectric materials: new approaches to an old problem. *Phys. Today* **1997,** 50 (3), 42-47.]

(2) Dresselhaus, M.S.; Chen, G.; Tang, M. Y.; Yang, R.; Lee, H.; Wang, D.; Ren, Z.; Fleurial, J.; Gogna, P. New directions for low-dimensional thermoelectric materials. *Adv. Mat.* **2007**, 1043-1054.

(3) DiSalvo, F. Thermoelectric cooling and power generation. *Science.* **1999,** 285, (30), 703-706.

(4) Hicks, L. D. Effect of quantum-well structures on the thermoelectric figure of merit. *Phys. Rev. B* **1993**, 727-729.

(5) Klemens, P. G. Thermal resistance due to point defects at high temperatures *Phys. Rev.* **1960**, 507-509.

(6) Meyyappan, M., *Carbon Nanotubes: Science and Applications*. CRC Press LLC: Florida, **2005**.

(7) Collines, P.G.; Bradley, K.; Ishigami, M.; Zettl, A. *Science.* **2000,** 287, (5459), 1801.

(8) Kaminishi, D.; Ozaki, H.; Ohno, Y.; Maehashi, K.; Inoue, Kazuhiko, K.; Matsumoto, K.; Seri, Y.; Masuda, A.; Matsumura, H. Air-stable n-type carbon nanotube field-effect transistors with Si3N4 passivation films fabricated by catalytic chemical vapor deposition. *Appl. Phys. Lett.* **2005,** 86.

(9) Kim, S.M.; Jang, J.H.; Kim, K. K.; Park, H. K.; Bae, J.J.; Yu, W. J.; Lee, I. H.; Kim, G.; Loc, D.D.; Kim, U. J.; Lee, E.; Shin, H.; Choi, J.; Lee, Y.H. Reduction-controlled viologen in bisolvent as an environmentally stable n-type dopant for carbon nanotubes. *J. Am. Chem. Soc.* **2008,** 131, (1), 327-331.

(10) Zhang, Z.; X. Liang, X.;Wang, S.; Yao, K.; Hu, Y.; Zhu, Y.; Chen, Q.; Zhou, W.; Li, Y.;Yao, Y.; Zhang, J.; Peng, L. Doping-free fabrication of carbon nanotube based ballistic cmos devices and circuits. *Nano Lett.* **2007,** 7, (12), 3603-3607.

(11) Shim, M.; Javey, A.; Kam, W.S.; Wong, N.; Hongjie Dai, H. Polymer functionalization for air-stable n-type carbon nanotube field-effect transistors. *J. Am. Chem. Soc.* **2001**, 11512-11513.

(12) Yamaguchi, I.; Yamamoto, T.; Soluble self-doped single-walled carbon nanotube. *Mat. Lett.* **2004,** 58, (5), 598-603.

(13) Li, Z.; Saini, V.; Dervishi, E.; Kunets, V. P.; Zhang, J.; Xu, Y.; Biris, A.R.; Salamo, G. J.; Biris, A.S. Polymer functionalized n-type single wall carbon nanotube photovoltaic devices. *Appl. Phys. Lett.* **2010,** 96, (3).

(14) Lin, Y.; Appenzeller, J.; Knoch, J.; Avouris, P. High-performance carbon nanotube field-effect transistor with tunable polarities. *IEEE Trans. on Nano. Tech.* **2005,** 4, (5), 481-489.

(15) Ryu, Y.; Freeman, D.; Yu, C. High electrical conductivity and n-type thermopower from double-/single-wall carbon nanotubes by manipulating charge interactions between nanotubes and organic/inorganic nanomaterials. *Carbon* **2011**, 49, (14), 4745-4751.

(16) Coleman, J.N.; Curran, S.; Dalton, A.B.; Davey, A.P.; McCarthy, B.; Blau, W.; Barklie, R.C. Percolation-dominated conductivity in a conjugated-polymer-carbon-nanotube composite. *Phys. Rev. B* **1998,** 58, (12), 7492-7495.

(17) Gojnya, F. H.; Wichmann, M. H. G.; Fiedler, B.; Kinloch, I.A.; Bauhofer, W.; Windle, A.H.; Schulte, K. Evaluation and identification of electrical and thermal conduction mechanisms in carbon nanotube/epoxy composites. *Polymer* **2006,** 47, (6), 2036-2048.

(18) Grunlan, J. C.; Mehrabi, A.R.; Bannon, M. V.; Bahr, J. L. Water-based single-walled-nanotube-filled polymer composite with an exceptionally low percolation threshold. *Adv. Mat.* **2004,** 16, (2), 150-153.

(19) Yu, C.; Choi, K.; Yin, L.; Grunlan, J. C. Light-weight flexible carbon nanotube based organic composites with large thermoelectric power factors. *ACS Nano* **2011**, 5, (10), 7885-7892.

(20) Mamedov, A. A.; Kotov, N. A.; Prato, M.; Guldi, D.M.; Wicksted, J. P.; Hirsch, A. Molecular design of strong single-wall carbon nanotube/polyelectrolyte multilayer composites. *Nature Mat.* **2002**, 1, (4), 190-194.

(21) Moore, V.C.; Strano, M.S.; Haroz, E. H.; Hauge, R.H.; Smalley, R. Individually suspended single walled carbon nanotubes in various surfactants. *Nano Lett.* **2003**, 3, (10) 1379-1382.

(22) Islam, M. F.; Rojas, E.; Bergey, D.M.; Johnson, A.T.; Yodh, A.G. High weight fraction surfactant solubilization of single-wall carbon nanotubes in water. *Nano Lett.* **2003,** 3, (2), 269-27

(23) Dillon, E. P.; Crouse. C. A.; Barron, A. R.; Synthesis, characterization, and carbon dioxide adsorption of covalently attached polyethyleneimine-functionalized single-wall carbon nanotubes. *ACS Nano.* **2008**, 2, (1), 156-164.

(24) Liao, K.; Wang, J.; Früchtl, D.; Alley, N. J.; Andreoli, E.; Dillon, E. P.; Barron, A. R.; Kim, H.; Byrne, H. J.; Blau, W. J.; Curran, S. A. Optical limiting study of double wall carbon nanotube–fullerene hybrids. *Chem. Phys. Lett.* **2010**, 489, 201-211.

(25) Muñoz, E.; Suh, D.; Collins, S.; Selvidge, M.; Dalton, A. B.; Kim, B. G.; Razal, J. M.; Ussery, G.; Rinzler, A.G.; Martìnez, M.T.; Baughman, R. H. Highly conducting carbon nanotube/ polyethyleneimine composite fibers. *Adv. Mat.* **2005**, 17, (8), 1064-1067.

(26) Chattopadhyay, D.; Galeska, I.; Papadimitrakopoulos, F. Complete elimination of metal catalysts from single wall carbon nanotubes. *Carbon* **2002,** 40, (7).

(27) Kim, D.; Kim, Y.; Choi, K.; Grunlan, J.C.; Yu, C. Improved Thermoelectric Behavior of Nanotube-Filled Polymer Composites with Poly(3,4-ethylenedioxythiophene) Poly(styrenesulfonate). *ACS Nano* **2010**, 4, (1), 513-523.

(28) Geng, Y.; Liu, M. Y.; Li, J.; Shi, X, M.; Kim, J. K. Effects of surfactant treatment on mechanical and electrical properties of CNT/epoxy nanocomposites. *Comp. A. Appl. Sci. and Manuf.* **2008**, 39, (12), 1876–1883.

(29) Kymakis, E.; Amaratunga, G. H. Electrical properties of single-wall carbon nanotube-polymer composite films. *J. Appl. Phys.* **2006**, 99, (8), 084302.

(30) Collines, P. G.; Bradley, K.; Ishigami, M.; Zettl, A. Extreme Oxygen Sensitivity of Electronic Properties of Carbon Nanotubes. *Science.* **2000**, 287, (5459), 1801-1804.

APPENDIX

This section contains supplemental figures and images collected from the experiments and a more complete table listing experimental conditions and results. Photographs of representative samples from each series are also included for the purpose of demonstrating the variability in film quality between the recipes.

Figures 19-21 were taken at the same time as Figure 11, which is a group of the images, one from each series, that were chosen as representative. The increase in surface roughness with a reduction in SDBS weight percent can be seen in these images as well, and in addition, one can see the variation in each sample due to random fracture events as well as the inhomogeneity in the composite due to poor dispersion and settling that occurred during drying.

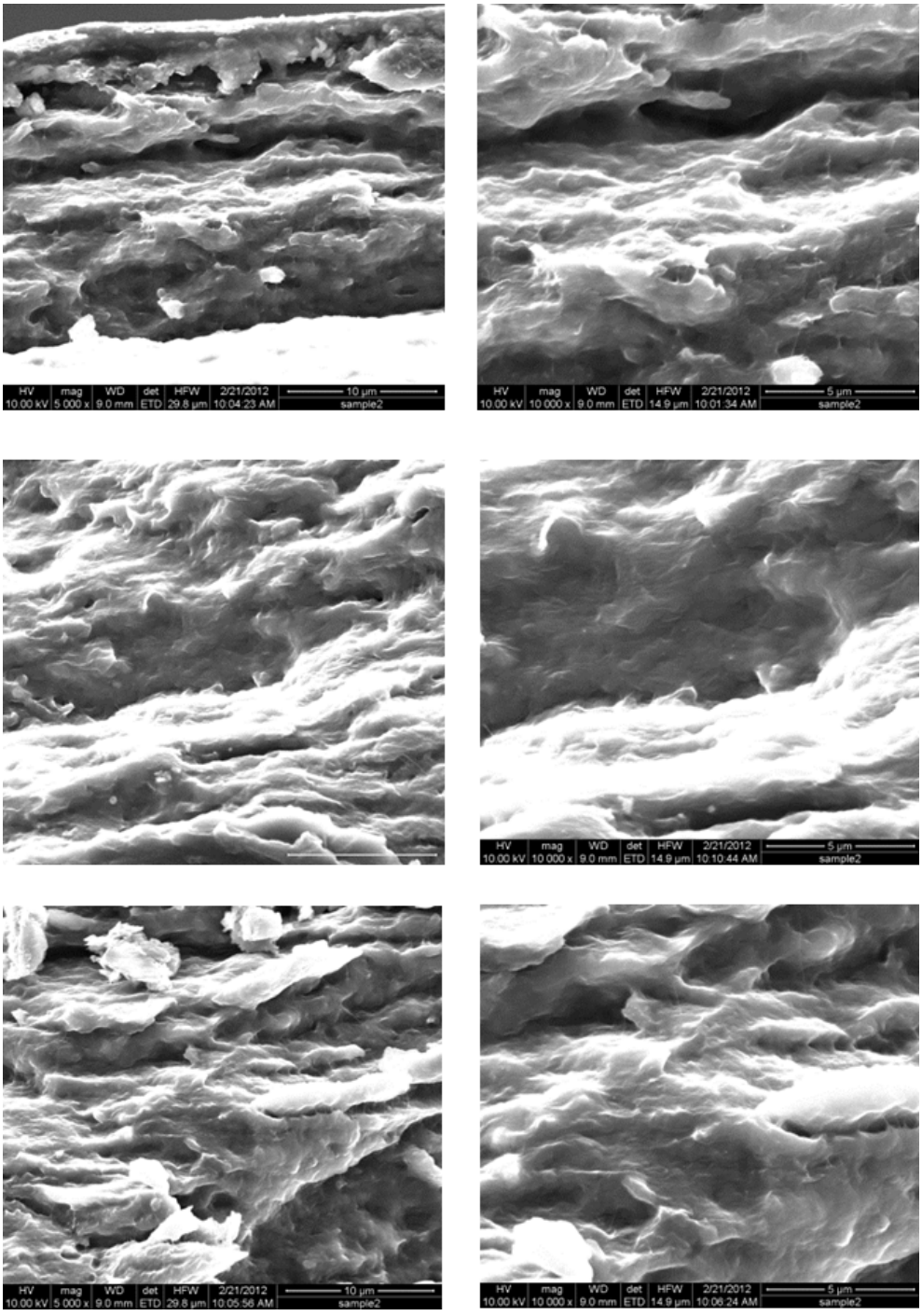

Figure 19. SEM images of sample composed of wt. percentages 20/60/10/10 for CNT/SDBS/PEI/PVAC. Scale bars on the top indicate 5 µm and 10 µm is indicated on the bottom row

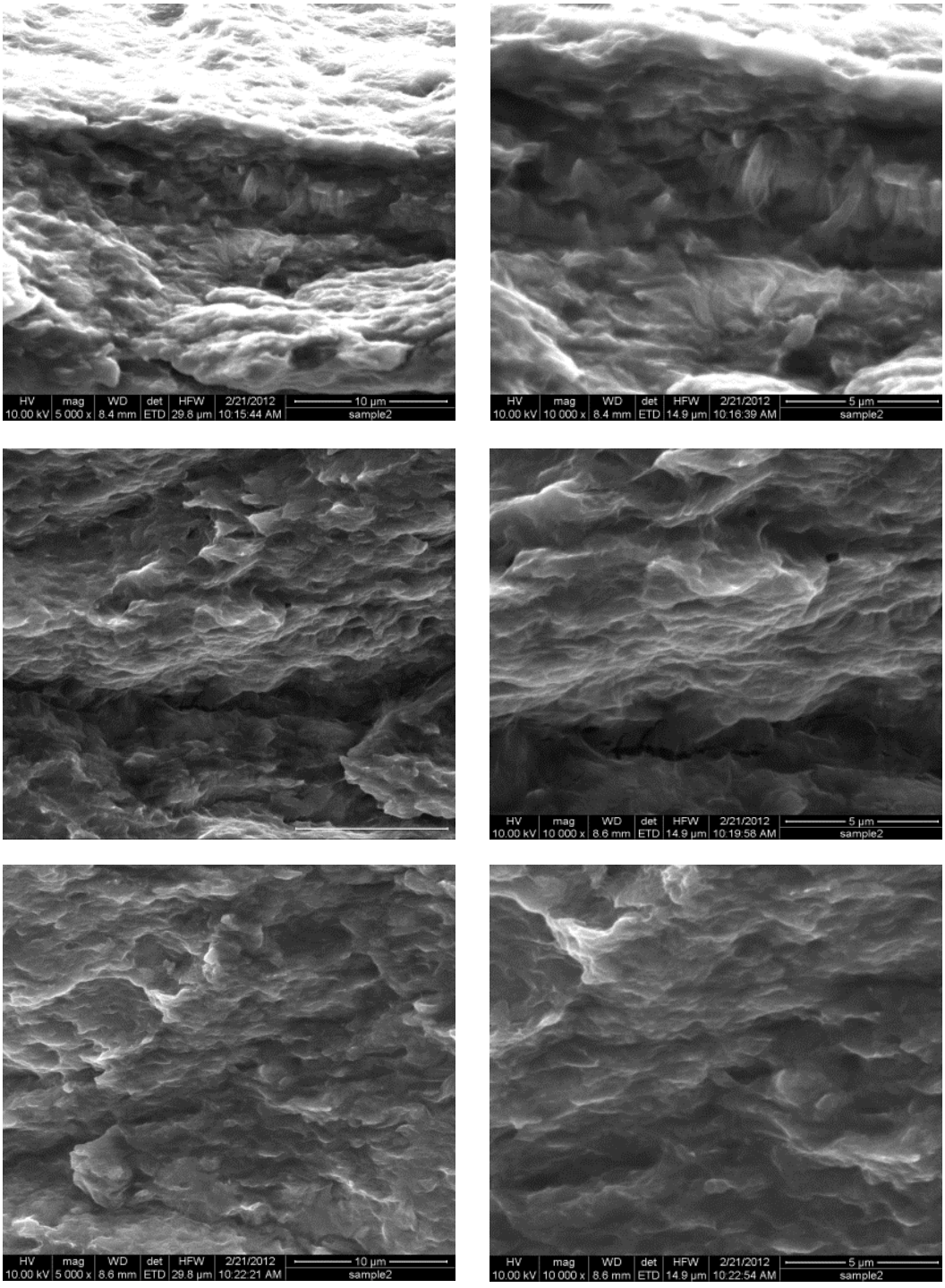

Figure 20. SEM images of sample composed of wt. percentages 20/40/10/30 for CNT/SDBS/PEI/PVAC. Scale bars indicate 10 µm on the left and 5 µm on the right.

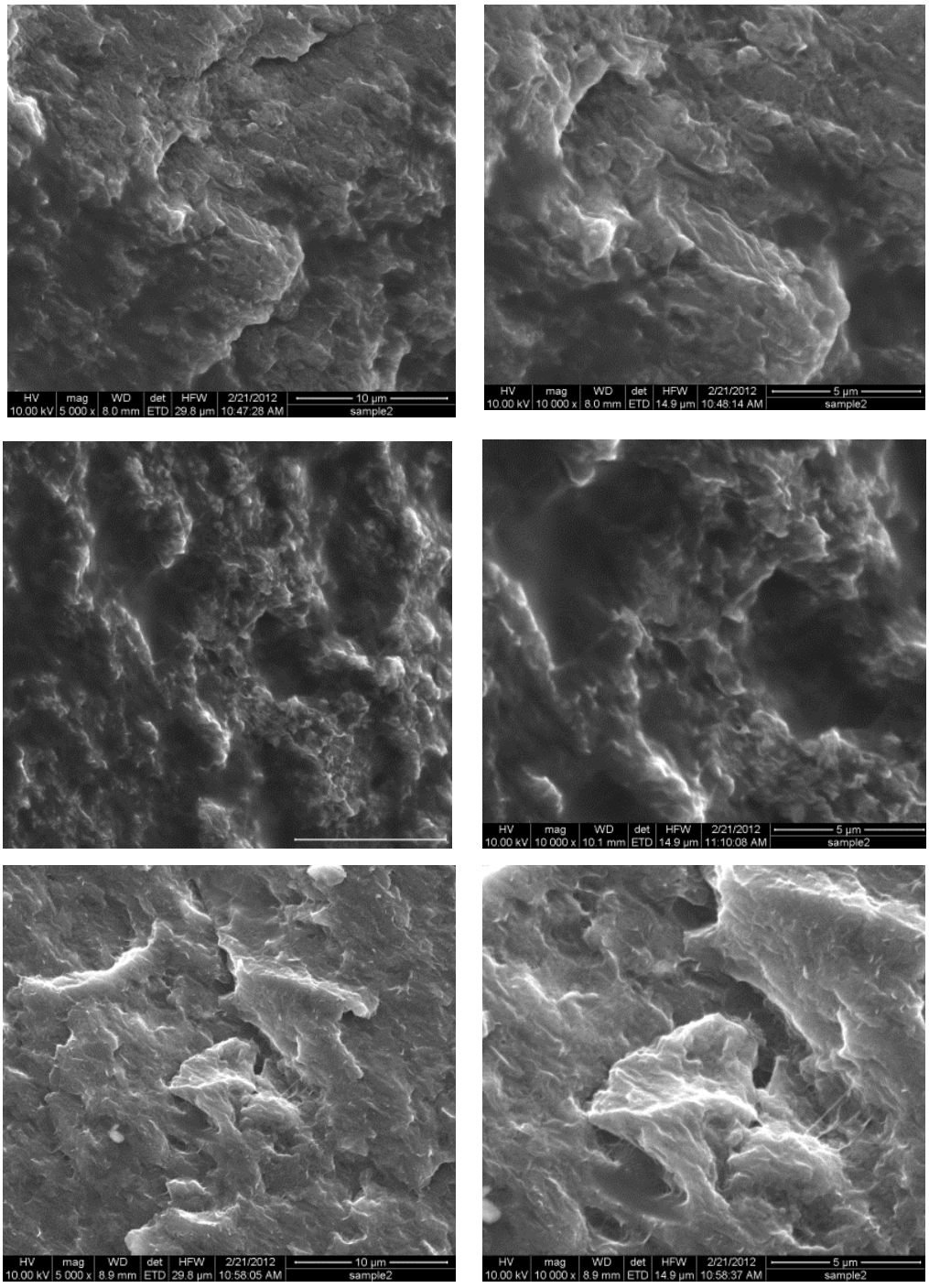

Figure 21. SEM images of sample composed of wt. percentages 20/20/10/50 for CNT/SDBS/PEI/PVAC Scale bars indicate 10 µm on the left and 5 µm on the right.

Figures 22-24 are photographs of the prepared films with the testing samples for each of the three series. Several of the samples, especially from the final two series, exhibit visible agglomerations which are believed to be composed largely of CNTs which were not well dispersed. These agglomerations tend to be associated with lower thermopowers and thermal conductivities.

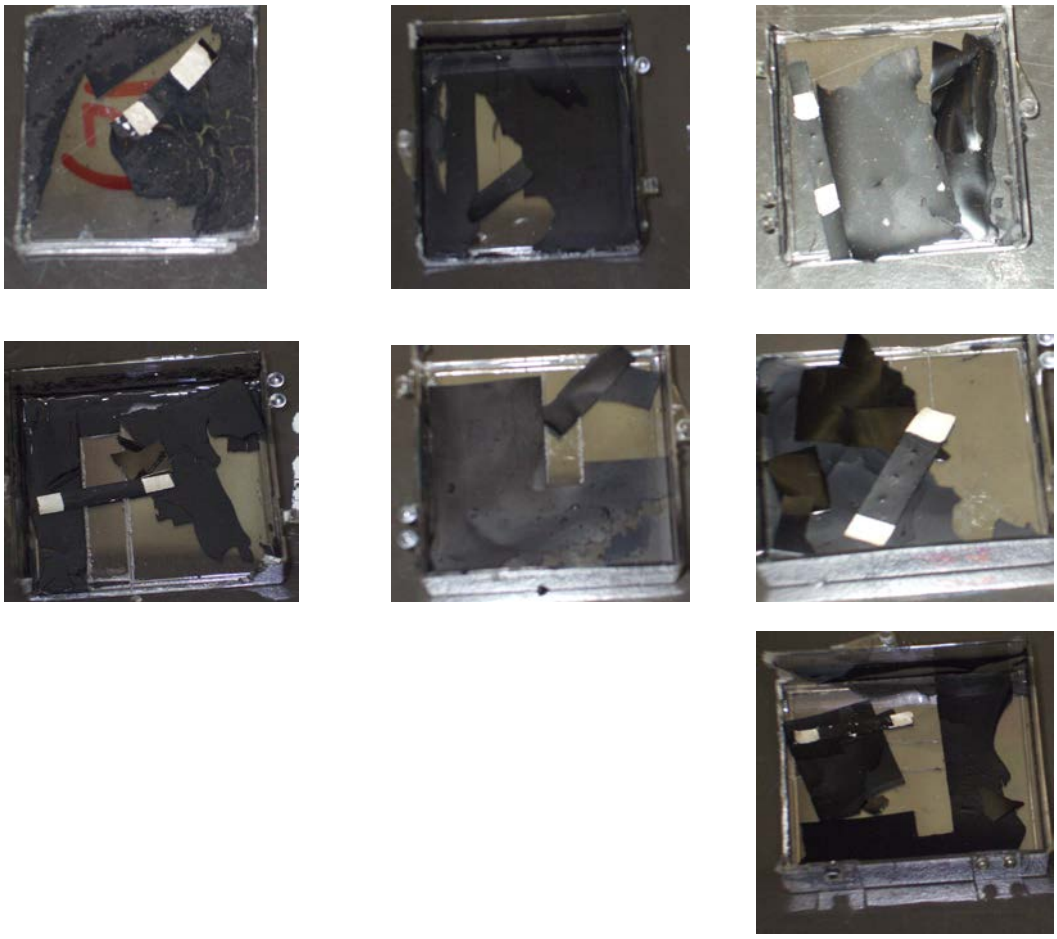

Figure 22. Photographs of typical samples from series one with SDBS weight percentages of 20 wt. % (left column) 40 wt. % (middle) and 60 wt. % (right).

Figure 23. Photographs of typical samples from series two with PEI weight percentages of (left to right) 10, 20 30, 40 and 50 wt. %.

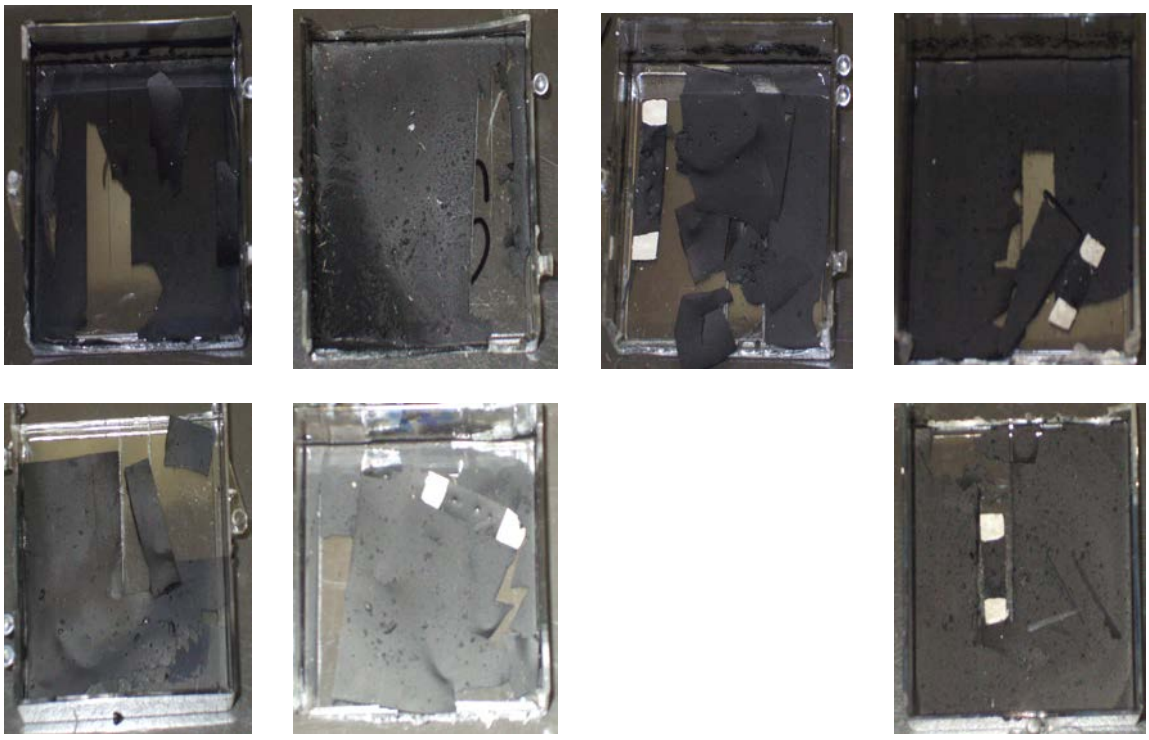

Figure 24. Photographs of typical samples from series three with PEI weight percentages of (left to right) 10, 20, 30 and 40 wt. %.

Table 2 is a summary of the preparation conditions and the results for the three series. The samples were not produced and tested in the order shown, as the different series were run several times with the different sonication and the two purities of CNTs. It should also be understood that in cases where a recipe can be part of two series, its information is copied in both places with a series specific name for ease of reference. The same test of the same prepared sample is meant, despite the fact that it appears in multiple locations, (see samples 1-1 and 2-3). In addition, please note that the negative thermopower values for all but sample 3-13 indicate successful n-type conversion. Lastly, for a few high performing samples, the experiment was repeated with the exact same preparation conditions. In these cases, the results are displayed in the graphs as error bars, whereas most of the bars are merely indicative of measurement error for the sample being studied.

Table 2 Summary of experimental procedures and results

Trial	CNT	SDBS	PEI	PVAC	Conductivity	Seebeck	Sonication	CNT Purity (%)
1-1	20	20	10	50	5.3133004	-5.3133	PEN	90
1-2	20	40	10	30	23	-24	PEN	90
1-3	20	60	10	10	120.24	-38.98	PEN	90
1-4	20	60	10	10	1479.09	-60.7	PEN	99
1-5	20	40	10	30	853.76	-75.9	PEN	99
1-6	20	20	10	50	427.39	-65.86	PEN	99
1-7	20	60	10	10	959	-82.8	PEN	99
1-8	20	60	10	10	1219.045	-71.75	PEN	99
2-1	20	20	40	100	21	-59	PEN	90
2-2	20	20	20	40	26	-41	PEN	90
2-3	20	20	10	50	5.3133004	-5.3133	PEN	90
2-4	20	20	5	55	9.426332	-36.88	PEN	90
2-5	20	20	40	20	1585	-82.1	BATH	99
2-6	20	20	50	10	954.18	-61.82	BATH	99
2-7	20	20	50	10	4.82	-62.81	BATH	99
2-8	20	20	50	10	756	-57.9	BATH	99
2-9	20	20	10	50	427.39	-65.86	PEN	99
2-10	20	20	20	40	388.67	-69.1	PEN	99
2-11	20	20	30	30	313.49	-72.41	PEN	99
2-12	20	20	40	20	415.13	-67.09	PEN	99
2-13	20	20	50	10	358.28	-69.19	PEN	99
3-1	20	40	10	90	23	-24	PEN	90
3-2	20	40	20	40	15.86	-84	PEN	90
3-3	20	40	30	50	2.05	-117	PEN	90
3-4	20	40	10	20	853.76	-75.9	PEN	99
3-5	20	40	20	10	582.6	-71.7	PEN	99
3-6	20	40	30	10	897.379562	-106.6	PEN	99
3-7	20	40	40	10	329.66	-100.73	PEN	99
3-8	20	40	40	50	635.3	-82.45	PEN	99
3-9	20	40	10	40	90.66	-63.14	BATH	99
3-10	20	40	40	30	348.57	-89.45	BATH	99
3-11	20	40	5	35	590.42	-97.68	BATH	99
3-12	20	40	1	39	500.06	-56.91	BATH	99
3-13	20	40	0.1	39.9	616.28	106.94	BATH	99

Finally, these last images are scanning electron micrographs of samples which possessed small differences in electrical properties. With the exception of Figure 25, they are less instructive on individually then they are on the aggregate. Of principle interest with Figure 25 is the atypical amount of CNTs pulled out of the polymer matrix. This sample, which was believed to be composed of 20/20/40/20 CNT/SDBS/PEI/PVAC wt. %, possessed properties which were atypically good for composites containing only 20 wt. % of CNTs. The images call this composition into question, as does the fact the subsequent attempts at replicating the properties have all failed.

The other images (Figure 26Figure 29) are mostly instructive in terms of the variation in micro scale structure that can be observed between samples which have similar electrical properties in addition to the variation that can be seen for samples of the same compositions.

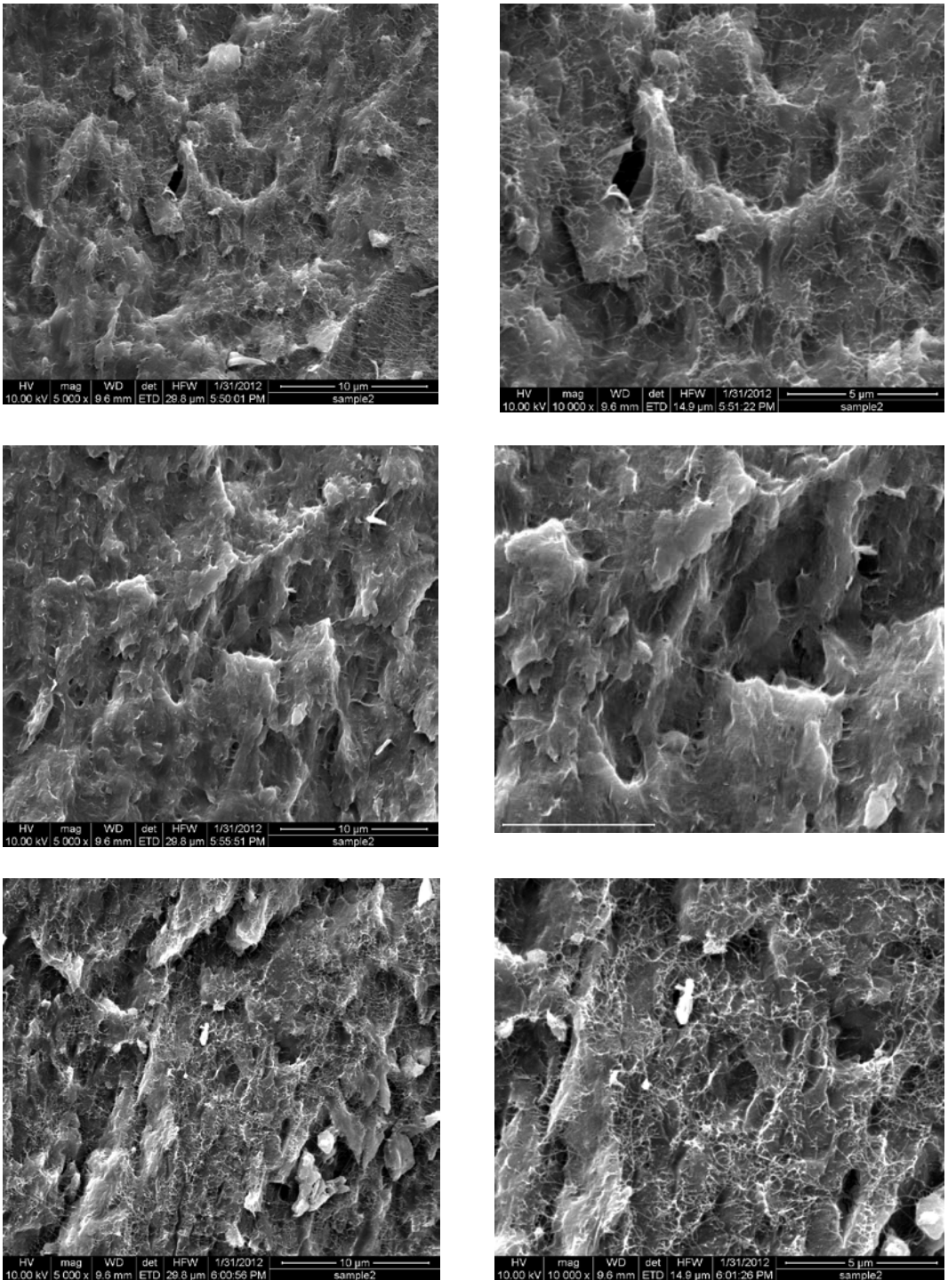

Figure 25. SEMs of sample once believed to be 20/20/40/20.

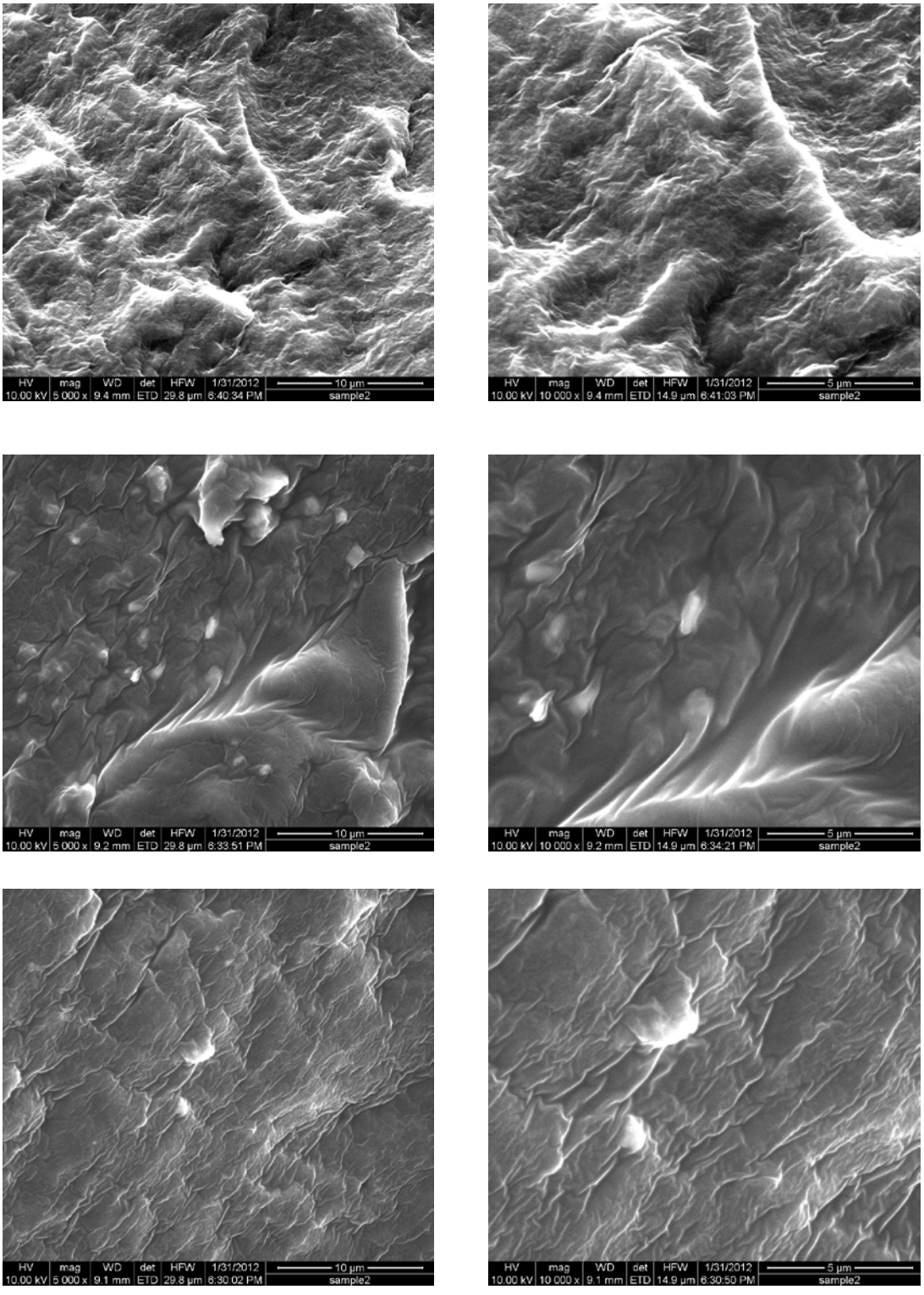

Figure 26. SEM of sample 2-6

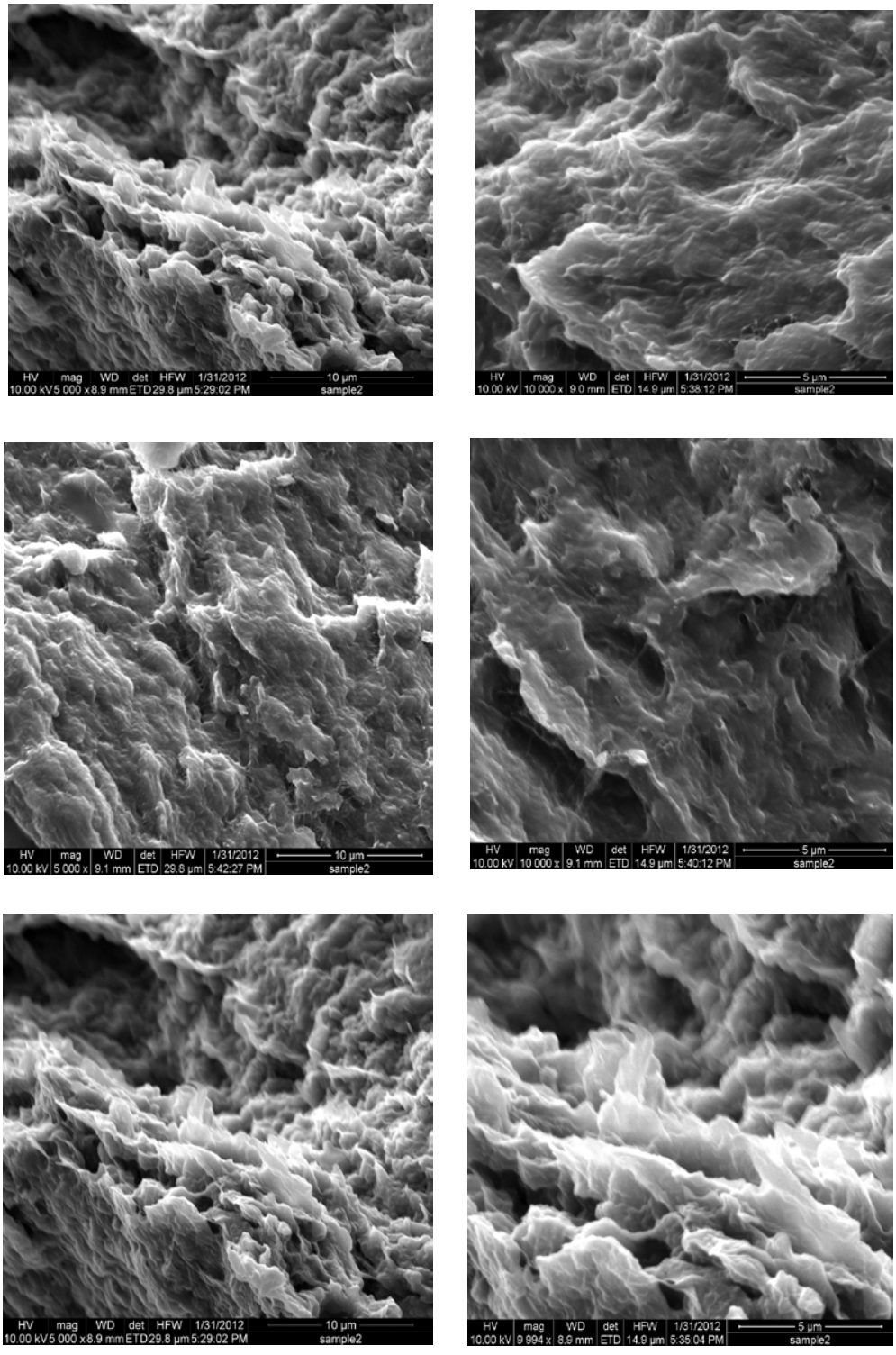

Figure 27. SEM Images of sample 2-11

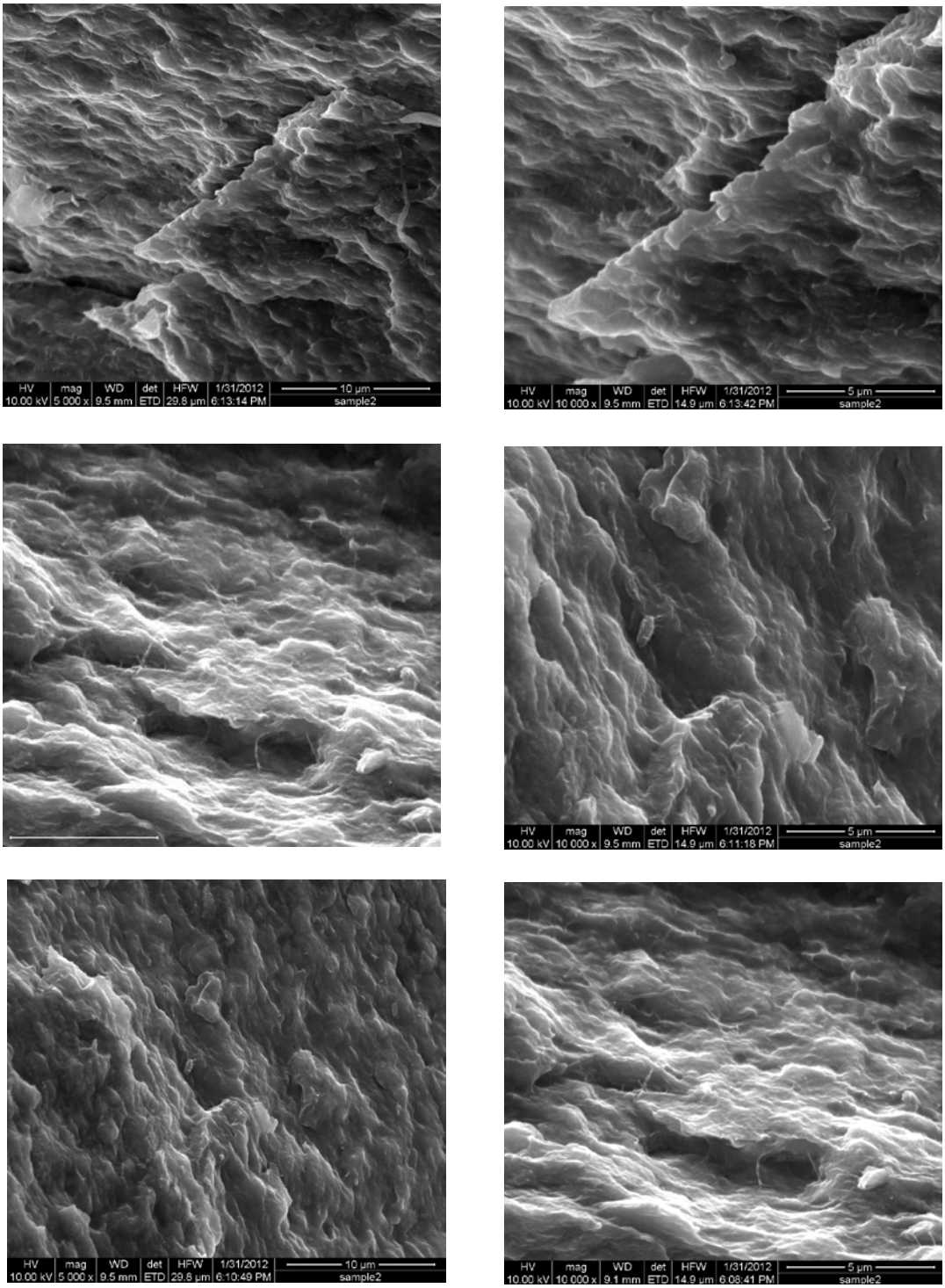

Figure 28. SEM images of Sample 3-5

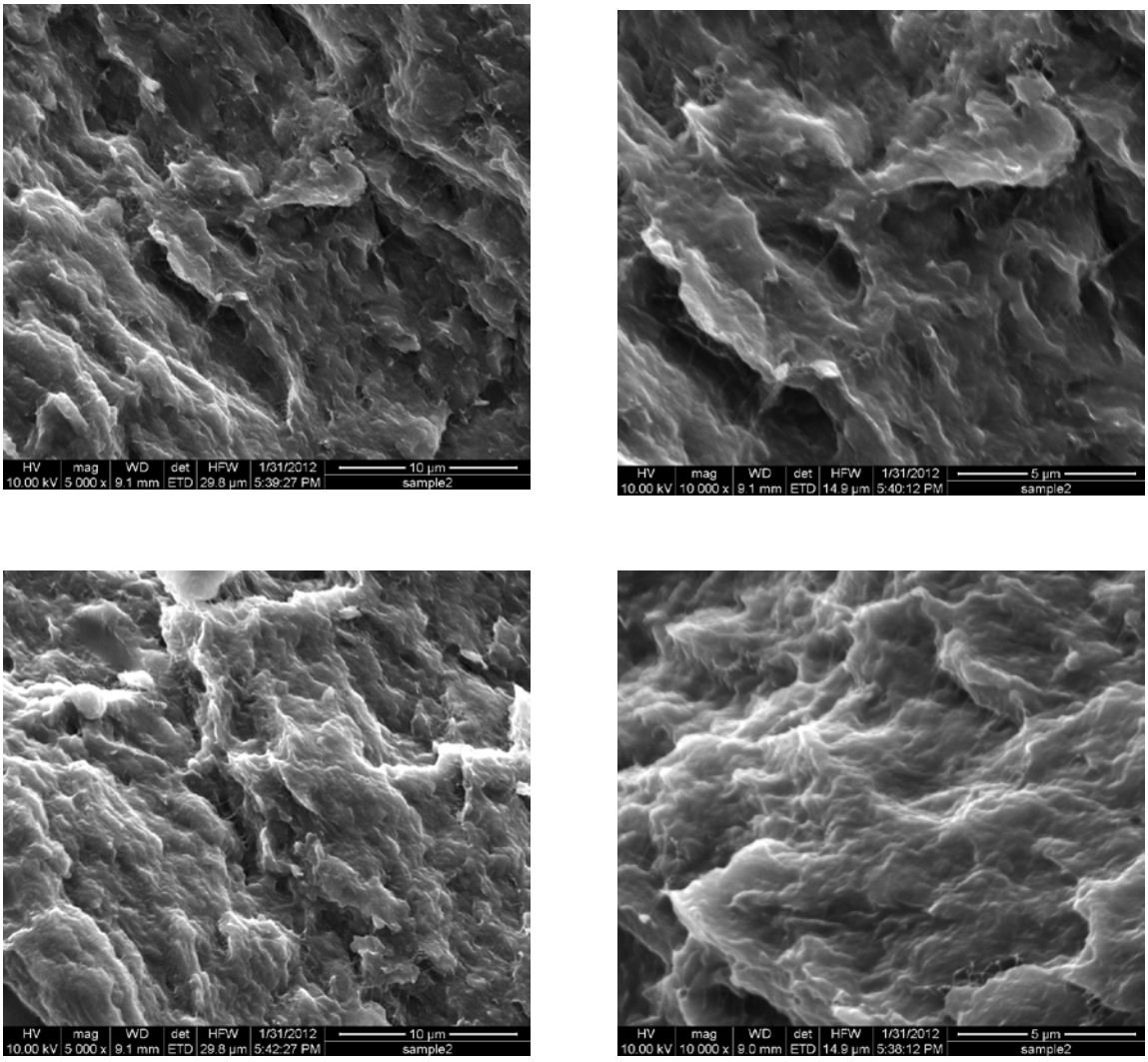

Figure 29. SEM images of sample 3-6

VITA

Dallas D. Freeman II received his Bachelor of Science in Mechanical Engineering from Brigham Young University in April 2010. He received his Master of Science in Mechanical Engineering from Texas A&M University in May 2012.

Mr. Freeman may now be reached at dustinmosspoint@gmail.com. His mailing address is:

17707 Moss Point Dr.

Spring, TX 77379